Fig. 10.23. We can approximate the volume of the central peak by $1/TW$. Thus, the height of the flat region must satisfy the equation

$$h \cdot 4WT + \frac{1}{WT} \simeq 1 \tag{153}$$

or

$$h \simeq \frac{1}{4WT}\left(1 - \frac{1}{WT}\right). \tag{154}$$

For large TW products,

$$h \simeq \frac{1}{4WT}. \tag{155}$$

This result gives us a general indication of the type of behavior we may be able to obtain. From the radar uncertainty principle, we know that this is the lowest *uniform* height we can obtain. Depressing certain areas further would require peaks in other areas.

With these four observations as background, we now try to find a waveform that leads to the ambiguity function in Fig. 10.23. In the absence of any obvious design procedure, a logical approach is to use the intuition we have gained from the few examples we have studied and the properties we have derived.

Barker Codes. A plausible first approach is to let N equal a small number and investigate all possible sequences of a_n. For example, if
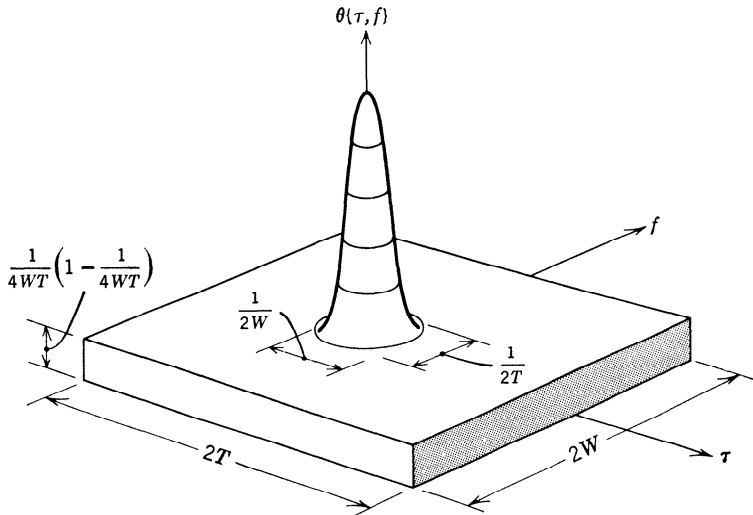

Fig. 10.23   A desirable ambiguity function.

$N = 3$, there are 2^3 arrangements. We can indicate the sequence by the amplitudes. Thus,

$$+ + - \tag{156}$$

denotes

$$\tilde{f}(t) = \frac{1}{\sqrt{3}} [u_1(t) + u_2(t) - u_3(t)]. \tag{157}$$

We can compute the correlation function $\phi(\tau, 0)$ easily. Since we are shifting rectangular pulses, we just compute

$$\phi(nT_s, 0), \qquad n = 1, 2, 3 \tag{158}$$

and connect these values with straight lines. The resulting correlation function is shown in Fig. 10.24. We see that the correlation function has the property that

$$|\phi(nT_s, 0)| \le \frac{1}{N}, \qquad n \ne 0. \tag{159}$$

Notice that the complement of this sequence, $- - +$, the reverse, $- + +$, and the complement of the reverse, $+ - -$, all have the same property. We can verify that none of the other sequences of length 3 has this property. Barker [17] developed sequences that satisfy the condition in (159) for various $N \le 13$. These sequences, which are referred to as Barker codes, are tabulated in Table 10.1. Unfortunately, Barker codes with lengths greater than 13 have not been found. It can be proved that no odd sequences greater than 13 exist and no even sequences with N between
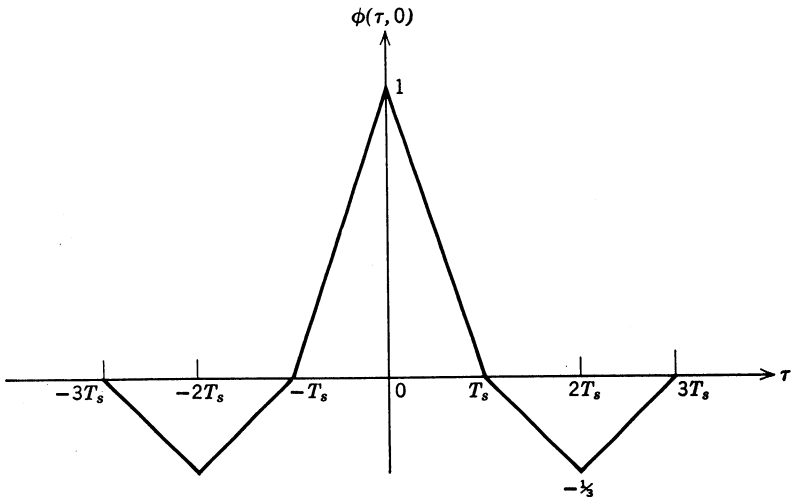

Fig. 10.24 **Correlation function of three-element Barker code.**

Table 10.1   Barker Sequences

N	Sequences
2	$+\,+,\,-\,+$
3	$+\,+\,-$
4	$+\,+\,-\,+,\,+\,+\,+\,-$
5	$+\,+\,+\,-\,+$
7	$+\,+\,+\,-\,-\,+\,-$
11	$+\,+\,+\,-\,-\,-\,+\,-\,-\,+\,-$
13	$+\,+\,+\,+\,+\,-\,-\,+\,+\,-\,+\,-\,+$

4 and 6084 have been found [18]. The magnitude of the time-frequency correlation function for a Barker code of length 13 is shown in Fig. 10.25. We see that there are two ridges of non-negligible height.

Shift-Register Sequences. A second approach to signal design is suggested by an example that is usually encountered in random-process courses. Consider the experiment of flipping a fair coin. If the outcome is a head, we let $a_1 = 1$. If the outcome is a tail, we let $a_1 = -1$. The nth toss determines the value of a_n. The result is a sample function, the familiar Bernoulli process. As $N \to \infty$, we have the property that

$$\phi(nT_s, 0) = 0, \qquad n \neq 0. \tag{160}$$

Thus, for large N, we would expect that the waveform would have a satisfactory correlation function. One possible disadvantage of this procedure is the storage requirement. From our results in Section 10.1, we know that the receiver must have available a replica of the signal in order to construct the matched filter. Thus, if $N = 1000$, we would need to store a sequence of 1000 amplitudes.
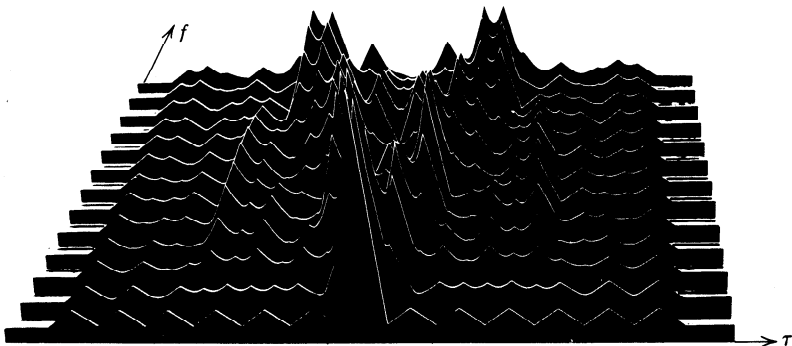

Fig. 10.25   Magnitude of time-frequency correlation function: Barker code of length 13 (From [19.])
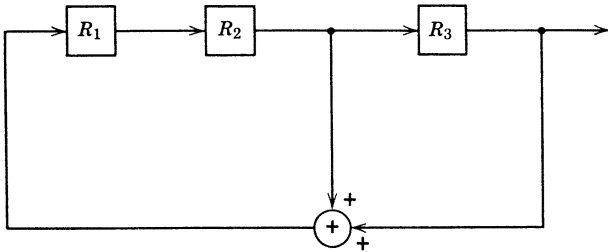
Fig. 10.26 Feedback shift register.

Fortunately, there exists a class of deterministic sequences that have many of the characteristics of Bernoulli sequences and can be generated easily. The device used to generate the sequence is called a *feedback shift register*. A typical three-stage configuration is shown in Fig. 10.26. Each stage has a binary digit stored in it. Every T_s seconds a clock pulse excites the system. Two operations then take place:

1. The contents shift one stage to the right. The digit in the last stage becomes the system output.

2. The output of various stages are combined using mod 2 addition. The output of these mod 2 additions is the new content of the first stage. In the system shown, the contents of stages 2 and 3 are added to form the input.

3. Since all of the operations are linear, we refer to this as a *linear shift register*.

The operation of this shift register is shown in detail in Table 10.2. We see that after the seventh clock pulse the contents are identical with

Table 10.2

	Contents			Output sequence						
Initial	1	1	1							
1	0	1	1	1						
2	0	0	1	1	1					
3	1	0	0	1	1	1				
4	0	1	0	0	1	1	1			
5	1	0	1	0	0	1	1	1		
6	1	1	0	1	0	0	1	1	1	
7	1	1	1	0	1	0	0	1	1	1
8										
9		↓				↓				
10	Repeats				Repeats					

the initial contents. Since the output is determined completely from the contents, the sequence will repeat itself. The period of this sequence is

$$L \triangleq 2^N - 1 = 7. \tag{161}$$

It is clear that we cannot obtain a sequence with a longer period, because there are only $2^N = 8$ possible states, and we must exclude the state 000. (If the shift register is in the 000 state, it continues to generate zeros.) Notice that we have chosen a particular feedback connection to obtain the period of 7. Other feedback connections can result in a shorter period.

To obtain the desired waveform, we map

$$\begin{cases} 1 \rightarrow +1, \\ 0 \rightarrow -1. \end{cases} \tag{162}$$

If we assume that the periodic sequence is *infinite* in extent, the correlation function can be computed easily. For convenience we normalize the energy per period to unity instead of normalizing the total energy. The correlation function of the resulting waveform is shown in Fig. 10.27. We see that

$$\phi_p(nT_s, 0) = \begin{cases} 1, & n = 0, L, 2L, \ldots \\ -\frac{1}{7}, & n \neq kL, \quad k = 0, 1, \ldots. \end{cases} \tag{163}$$

All our comments up to this point pertain to the three-stage shift register in Fig. 10.26. In the general case we have an N-stage shift register.
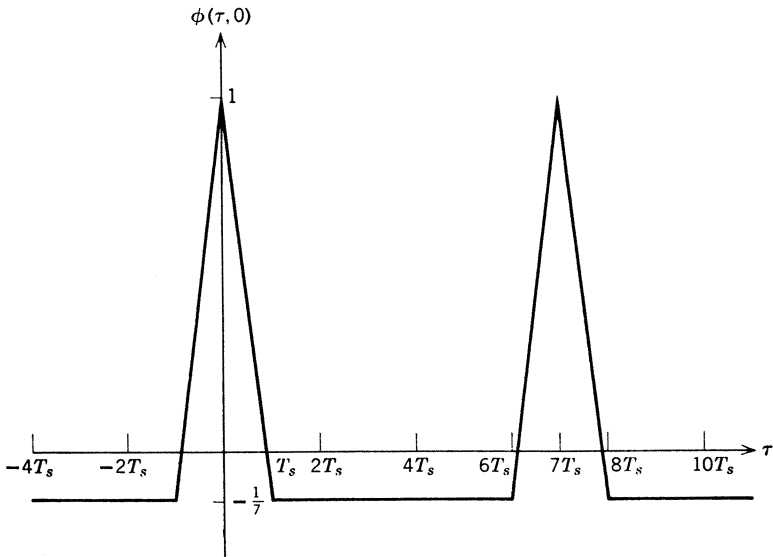

Fig. 10.27 Correlation function of a periodic pseudorandom sequence.

Since there are 2^N states, we cannot generate a sequence whose period is greater than $2^N - 1$. However, it is not clear that there exists a feedback configuration that will generate a sequence of this period. To prove the existence of such a sequence and find the configuration that produces one requires mathematical background that we have not developed. The properties of shift-register sequences have been studied extensively by Golomb, [20], Huffman [21], Zierler [22], Peterson [23], and Elspas [24]. Very readable tutorial discussions are given by Ristenblatt [25], [26] and Golomb [27, Chapters 1 and 2]. The result of interest to us is that for all N there exists at least one feedback connection such that the output sequence will have a period

$$L = 2^N - 1. \tag{164}$$

These sequences are called *maximal-length shift-register* sequences. Notice that the length is an exponential function of the number of stages. A list of connections for $N \leq 31$ is given by Peterson [23]. A partial list for $N \leq 6$ is given in Problems 10.4.5 and 10.4.6. These sequences are also referred to as *pseudo-random (PR) sequences*. The "random" comes from the fact that they have many of the characteristics of a Bernoulli sequence, specifically the following:

    1. In a Bernoulli sequence, the number of ones and zeros is approximately equal. In a PR sequence, the number of ones per period is one more than the number of zeros per period.

    2. A run of a length n means that we have n consecutive outputs of the same type. In a Bernoulli sequence, approximately half the runs are of length 1, one-fourth of length 2, one-eighth of length 3, and so forth. The *PR* sequences have the same run characteristics.

    3. The autocorrelation functions are similar.

The "pseudo" comes from the fact that the sequences are perfectly deterministic. The correlation function shown in Fig. 10.27 assumes that the sequence is periodic. This assumption would be valid in a continuous-wave (CW) radar. Applications of this type are discussed in [28] and [29]. Continuous PR sequences are also used extensively in digital communications. In many radar systems we transmit one period of the sequence. Since the above properties assumed a periodic waveform, we must evaluate the behavior for the truncated waveform. For small N, the correlation function can be computed directly (e.g., Problem 10.4.3). We can show that for large N the sidelobe levels on the τ-axis approaches $\sqrt{N}$ (or $\sqrt{WT}$). The time-frequency correlation function can be obtained experimentally.
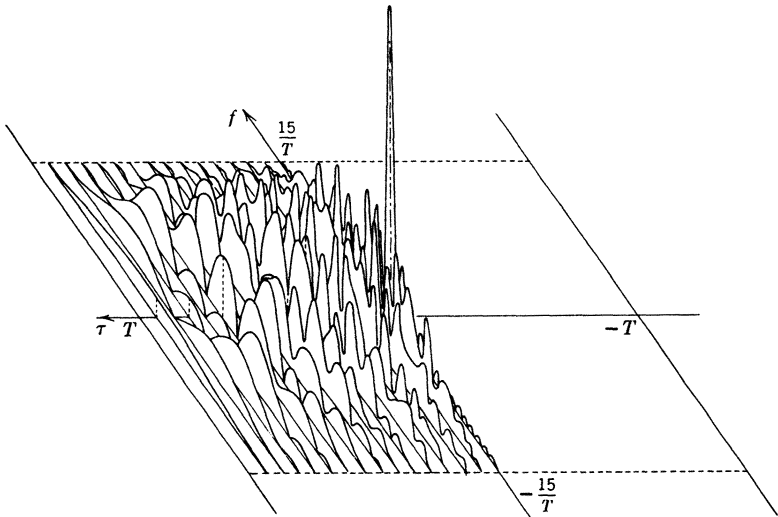
Fig. 10.28 $|\phi\{\tau, f\}|$ **for pseudorandom sequence of length** $N = 15$ **(From [35]).**

A plot for $N = 15$ is shown in Fig. 10.28. In many applications, the detailed structure of $\phi\{\tau, f\}$ is not critical. Therefore, in most of our discussion we shall use the approximate function shown in Fig. 10.29. This function has the characteristics hypothesized on page 316. Thus, it appears that the shift-register sequences provide a good solution to the combined ambiguity and accuracy problem.
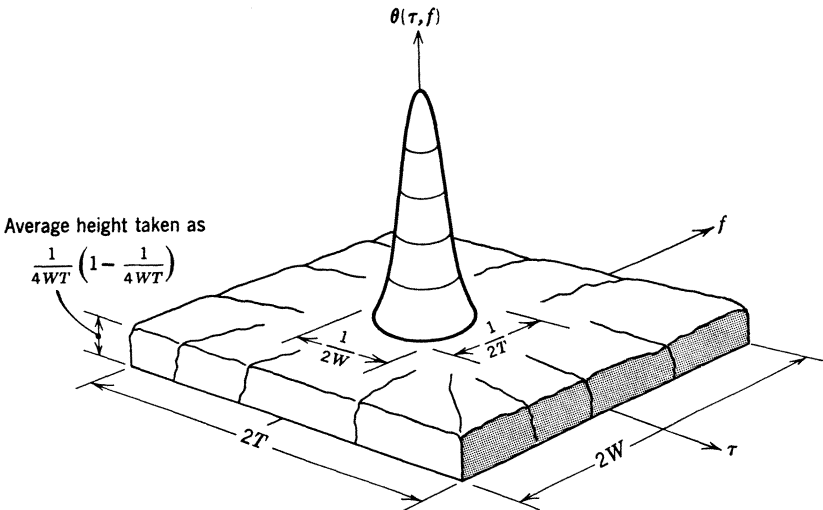

Fig. 10.29 **Approximation to the ambiguity function of a pseudorandom sequence.**

10.4.3 Other Coded Sequences

Before leaving our discussion of coded pulse sequences, we should point out that there are several alternatives that we have not discussed. The interested reader can consult [14, Chapter 8] and [30] for a tutorial discussion, or the original papers by Huffman [31], Golomb and Scholtz [32], Heimiller [33], and Frank [34].

We should emphasize that pulse sequences are frequently used in practice because they are relatively easy to generate, the optimum receiver is relatively easy to implement, and they offer a great deal of flexibility. Readers who are specializing in radar signal design should spend much more time on the study of these waveforms than our general development has permitted.

Up to this point we have assumed that only a single target is present. In many cases, additional targets interfere with our observation of the desired target. This problem is commonly called the resolution problem. We discuss it in the next section.

10.5 RESOLUTION

The resolution problem in radar or sonar is the problem of detecting or estimating the parameters of a desired target in the presence of other targets or objects that act as reflectors. These reflectors may be part of the environment (e.g., other airplanes, missiles, ships, rain) or may be deliberately placed by an enemy to cause confusion (e.g., decoys, electronic countermeasures, or chaff). It is convenient to divide the resolution
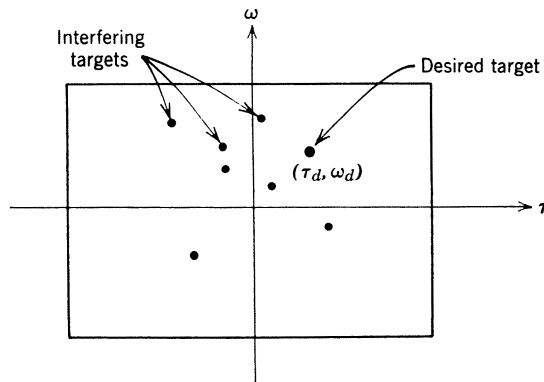

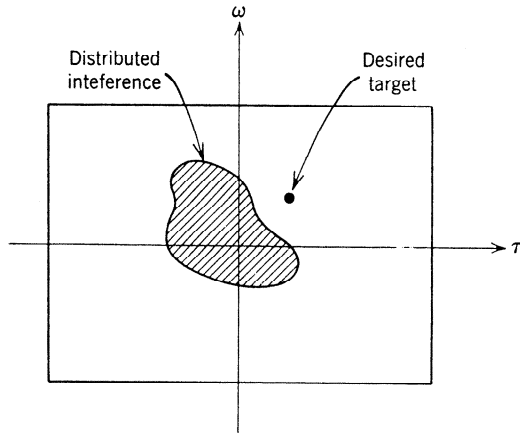**Fig. 10.30** **Target geometry for discrete resolution problem.**

Fig. 10.31 Geometry for continuous resolution problem.

problem into two categories:

1. Resolution in a discrete environment.
2. Resolution in a continuous (or dense) environment.

We now discuss our model for these two categories.

In Figure 10.30, we show the region of the τ, ω plane that we must investigate. The desired target is at coordinates τ_d, ω_d. A set of K interfering targets are at various points in the τ, ω plane. The desired and interfering targets are assumed to be slowly fluctuating Rayleigh targets. In general, the strengths of the various targets may be unequal. (Unfortunately, we occasionally encounter the problem in which the interfering target strengths are appreciably larger than the desired target strength.) We shall give a detailed model for the discrete resolution problem in the next section.

In the continuous resolution problem, the interference is modeled as a continuum of small reflectors distributed over some area in the τ, ω plane, as shown in Fig. 10.31. This model is appropriate to the reverberation problem in sonar and the clutter problem in radar. We whall discuss it in more detail in Chapter 13 as part of our discussion of distributed targets.

We now consider the discrete resolution problem in detail.

10.5.1 Resolution In a Discrete Environment: Model

In this section, we consider a typical resolution problem. The particular example that we shall discuss is a *detection* problem, but similar results can be obtained for estimation problems.

We want to decide whether or not a target is present at a particular point (τ_d, ω_d) in the τ, ω plane. For algebraic simplicity, we let

$$\tau_d = 0 \tag{165}$$

and

$$\omega_d = 0. \tag{166}$$

There are two sources of interference:

1. Bandpass white noise with spectral height $N_0/2$.
2. A set of K interfering targets located at (τ_i, ω_i), $i = 1, 2, \ldots, K$. We model these targets as slowly fluctuating point targets whose location and average strength are known. The fact that exactly K interfering targets are present is also assumed to be known.

The transmitted signal is

$$s_t(t) = \sqrt{2E_t} \, \mathrm{Re} \, [\tilde{f}(t)e^{j\omega_c t}], \tag{167}$$

where $\tilde{f}(t)$ is the normalized complex envelope.

The complex envelope of the received signal on H_0 is

$$\tilde{r}(t) = \sqrt{E_t} \left[\sum_{i=1}^{K} \tilde{b}_i \tilde{f}(t - \tau_i)e^{j\omega_i t} \right] + \tilde{w}(t), \qquad -\infty < t < \infty : H_0. \tag{168}$$

When the desired target is present, the complex envelope is

$$\tilde{r}(t) = \sqrt{E_t} \left[\tilde{b}_d \tilde{f}(t) + \sum_{i=1}^{K} \tilde{b}_i \tilde{f}(t - \tau_i)e^{j\omega_i t} \right] + \tilde{w}(t), \qquad -\infty < t < \infty : H_1. \tag{169}$$

The multipliers $\tilde{b}_d$ and $\tilde{b}_i$ are zero-mean complex Gaussian variables that are statistically independent with unequal variances:

$$E[\tilde{b}_d \tilde{b}_d^*] = 2\sigma_d^2, \tag{170}$$

$$E[\tilde{b}_i \tilde{b}_j^*] = 2\sigma_i^2 \, \delta_{ij}, \qquad i, j = 1, 2, \ldots, K, \tag{171}$$

and

$$E[\tilde{b}_d \tilde{b}_d] = E[\tilde{b}_i \tilde{b}_i] = E[\tilde{b}_d \tilde{b}_i^*] = E[\tilde{b}_d \tilde{b}_i] = 0, \qquad i = 1, \ldots, K. \tag{172}$$

There are several issues of interest with respect to this model. The first two concern the receiver design, and the next two concern the signal design.

1. We might assume that the receiver is designed *without* knowledge of the interfering signals. The resulting receiver will be the bandpass matched filter that we derived previously. We can then compute the effect of the

interfering targets on the receiver performance. We refer to this as the *conventional* receiver problem.

2. We can design the receiver using the assumed statistical properties of the interference. We shall see that this is a special case of the problem of detection in colored bandpass noise that we discussed in Section 9.3. We refer to this as the optimum receiver problem.

3. We can require the receiver to be a matched filter (as in part 1) and then choose $\tilde{f}(t)$ to minimize the interference effects.

4. We can use the optimum receiver (as in part 2) and choose the signal to minimize the interference effects.

We now discuss these four issues.

10.5.2   Conventional Receivers

The performance of the conventional receiver can be obtained in a straightforward manner. If we use a bandpass filter matched to $\tilde{f}(t)$, the optimum receiver performs the test

$$|\tilde{l}_{wo}|^2 \triangleq \left| \int_{-\infty}^{\infty} \tilde{r}(t)\tilde{f}^*(t)\, dt \right|^2 \underset{H_0}{\overset{H_1}{\gtrless}} \gamma \tag{173}$$

[see (9.36) and (9.39).] We use the subscript *wo* to indicate that the test would be *optimum* if the noise were *white*. Now, since $\tilde{l}_{wo}$ is a complex Gaussian variable under both hypotheses, the performance is completely determined by

$$\Delta_{wo} \triangleq \frac{E[|\tilde{l}_{wo}|^2 \mid H_1] - E[|\tilde{l}_{wo}|^2 \mid H_0]}{E[|\tilde{l}_{wo}|^2 \mid H_0]} \tag{174}$$

[see (9.49).] To evaluate the two expectations in (174), we substitute (168) and (169) into the definition in (173). The denominator in (174) is

$$E[|\tilde{l}_{wo}|^2|H_0] = E\left\{ \int_{-\infty}^{\infty} \left[\sqrt{E_t} \sum_{i=1}^{K} \tilde{b}_i \tilde{f}(t - \tau_i)e^{j\omega_i t} + \tilde{w}(t) \right] \tilde{f}^*(t)\, dt \right.$$

$$\left. \times \int_{-\infty}^{\infty} \left[\sqrt{E_t} \sum_{k=1}^{K} \tilde{b}_k^* \tilde{f}^*(u - \tau_k)e^{-j\omega_k u} + \tilde{w}^*(u) \right] \tilde{f}(u)\, du \right\}. \tag{175}$$

Using the independence of the $\tilde{b}_i$ and the definition in (18), this reduces to

$$E[|\tilde{l}_{wo}|^2 \mid H_0] = \sum_{i=1}^{K} \bar{E}_{r_i}\theta(\tau_i, \omega_i) + N_0, \tag{176}$$

where

$$\bar{E}_{r_i} \triangleq 2E_t\sigma_i^2 \tag{177}$$

is the average energy received from the ith interfering target. Similarly,

$$E[|\bar{l}_{wo}|^2 \mid H_1] - E[|\bar{l}_{wo}|^2 \mid H_0] = \bar{E}_{r_d}, \tag{178}$$

where

$$\bar{E}_{r_d} \triangleq 2E_t\sigma_d^2 \tag{179}$$

is the average received energy from the desired target. Then

$$\boxed{\Delta_{wo} = \frac{\dfrac{\bar{E}_{r_d}}{N_0}}{1 + \displaystyle\sum_{i=1}^{K} (\bar{E}_{r_i}/N_0)\theta(\tau_i, w_i)}.} \tag{180}$$

The numerator corresponds to the performance when only white noise is present. The second term in the denominator represents the degradation in the performance due to the interfering targets. We see that the performance using the conventional matched filter is completely characterized by the average strength of the return from the interfering targets and the value of the ambiguity function at their delay and Doppler location.

Conceptually, at least, this result provides the answer to the third issue. We design a signal whose ambiguity function equals zero at the K points in the τ, ω plane where the interfering signals lie. Even if we could carry out the design, several practical difficulties remain with the solution:

1. The resulting waveform will undoubtedly be complicated.

2. Each time the environment changes, the transmitted signal will have to change.

3. The performance may be sensitive to the detailed assumptions of the model (i.e., the values of τ_i and ω_i).

On the other hand, there are a number of physical situations in which our solution gives a great deal of insight into how to design good signals. A simple example illustrates the application of the above results.

Example. Consider the multiple-target environment shown in Fig. 10.32. We are interested in detecting zero-velocity targets. The interfering targets are moving at a velocity such that there is a *minimum* Doppler shift of ω_0. We want to design a signal such that

$$\theta(\tau, \omega) = 0, \qquad |\omega| > \omega_0. \tag{181}$$

We could accomplish this exactly by transmitting

$$\tilde{f}(t) = \sqrt{\frac{4\pi}{\omega_0}} \frac{\sin \omega_0 t}{t}. \tag{182}$$

This result can be verified by looking at the ambiguity function of the rectangular pulse in Example 1 (page 280) and using the duality result in Property 6 (pages 309–310).
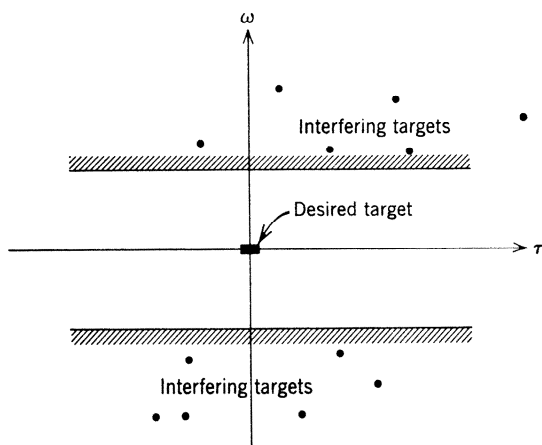
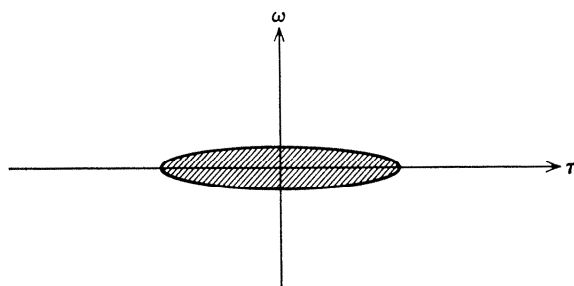**Fig. 10.32   Multiple-target geometry.**

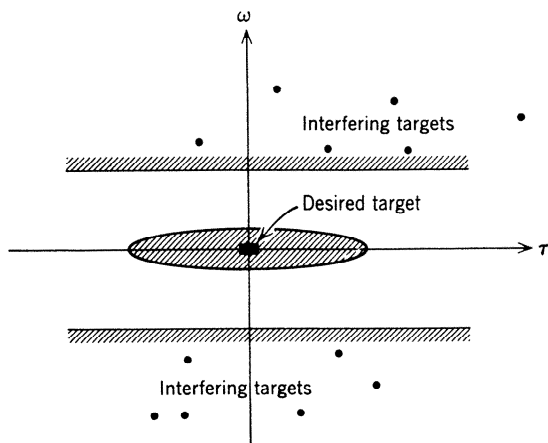**Fig. 10.33   Contour of ambiguity function of rectangular pulse.**

Fig. 10.34   Signal-interference relation.

On the other hand, we can make

$$\theta(\tau, \omega) \simeq 0, \qquad |\omega| > \omega_0 \tag{183}$$

by transmitting

$$\tilde{f}(t) = \begin{cases} \dfrac{1}{\sqrt{T}}, & 0 \le t \le T, \\[2mm] 0, & \text{elsewhere}, \qquad T \gg \dfrac{2\pi}{\omega_0}. \end{cases} \tag{184}$$

This solution is more practical. A typical contour of the resulting ambiguity function is given in Fig. 10.33, and is shown superimposed on the interference plot in Fig. 10.34. The reason for this simple solution is that the interference and desired targets have some separation in the delay-Doppler plane. If we had ignored the resolution problem, we might have used some other signal, such as a short pulse or a PR waveform. In the target environment shown in Fig. 10.32, the interfering targets can cause an appreciable degradation in performance.

The result of this example suggests the conclusion that we shall probably reach with respect to signal design. No single signal is optimum from the standpoints of accuracy, ambiguity, and resolution under all operating conditions. The choice of a suitable signal will depend on the anticipated target environment.

Now we turn to the second issue. Assuming that we know the statistics of the interference, how do we design the optimum receiver?

10.5.3 Optimum Receiver: Discrete Resolution Problem

Looking at (168) and (169), we see that the sum of the returns from the interfering targets can be viewed as a sample function from complex Gaussian noise processes. If we denote the first term in (168) as $\tilde{n}_c(t)$, then

$$\tilde{n}_c(t) = \sqrt{E_t} \left[\sum_{i=1}^{K} \tilde{b}_i \tilde{f}(t - \tau_i) e^{j\omega_i t} \right], \tag{185}$$

and we have the familiar problem of detection in nonwhite complex Gaussian noise (see Section 9.3). The covariance function of $\tilde{n}_c(t)$ is

$$\tilde{K}_c(t, u) = \sum_{i=1}^{K} \bar{E}_{r_i} \tilde{f}(t - \tau_i) \tilde{f}^*(u - \tau_i) e^{j\omega_i(t-u)}, \qquad -\infty < t, u < \infty. \tag{186}$$

We have used an infinite observation for algebraic simplicity. Usually $\tilde{f}(t)$ has a finite duration, so that $\tilde{K}_c(t, u)$ will be zero outside some region in the (t, u) plane. From (9.69), the optimum receiver performs the operation

$$\left| \int_{T_i}^{T_f} \tilde{r}(t) \tilde{g}^*(t) \, dt \right|^2 \gtrless \gamma, \tag{187}$$
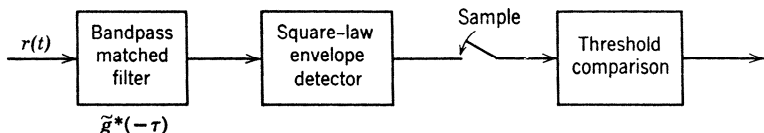
Fig. 10.35   Optimum receiver.

where $g(t)$ satisfies (9.74). To find $\tilde{f}(t)$, we substitute (188) into (9.74). The result is

$$\tilde{f}(t) = \int_{-\infty}^{\infty} \left[\sum_{i=1}^{K} \bar{E}_{r_i}\tilde{f}(t - \tau_i)\tilde{f}^*(u - \tau_i)e^{j\omega_i(t-u)} \right] \tilde{g}(u)\,du + N_0\tilde{g}(t),$$

$$-\infty < t < \infty. \quad (188)$$

We see that this is an integral equation with a separable kernel (see pages I-322–I-325). It can be rewritten as

$$\tilde{f}(t) = \sum_{i=1}^{K} \bar{E}_{r_i}\tilde{f}(t - \tau_i)e^{j\omega_i t} \left(\int_{-\infty}^{\infty} \tilde{f}^*(u - \tau_i)e^{-j\omega_i u}\tilde{g}(u)\,du \right) + N_0\tilde{g}(t),$$

$$-\infty < t < \infty. \quad (189)$$

The solution to (189) is

$$\tilde{g}(t) = \tilde{g}_d\tilde{f}(t) + \sum_{i=1}^{K} \tilde{g}_i\tilde{f}(t - \tau_i)e^{j\omega_i t}, \qquad -\infty < t < \infty, \quad (190)$$

where $\tilde{g}_d$ and $\tilde{g}_i$, $i = 1, \ldots, K$, are constants that we must find. The optimum receiver is shown in Fig. 10.35. The calculation of the constants is a straightforward but tedious exercise in matrix manipulation. Since this type of manipulation arises in other situations, we shall carry out the details. The results are given in (201) and (202).

Calculation of Filter Coefficients. We first define four matrices. The coefficient matrix $\tilde{\mathbf{b}}$ is

$$\tilde{\mathbf{b}} \triangleq \begin{bmatrix} \tilde{b}_1 \\ \tilde{b}_2 \\ \cdot \\ \cdot \\ \cdot \\ \tilde{b}_K \end{bmatrix}. \quad (191)$$

The interference matrix $\tilde{\mathbf{f}}_I(t)$ is

$$
\tilde{\mathbf{f}}_I(t) \triangleq \begin{bmatrix} \tilde{f}(t - \tau_1)e^{j\omega_1 t} \\ \tilde{f}(t - \tau_2)e^{j\omega_2 t} \\ \cdot \\ \cdot \\ \cdot \\ \tilde{f}(t - \tau_K)e^{j\omega_K t} \end{bmatrix}. \tag{192}
$$

In addition, we define

$$
\tilde{\boldsymbol{\Lambda}} \triangleq E_t[E[\tilde{\mathbf{b}}\tilde{\mathbf{b}}^\dagger]] = 2E_t \begin{bmatrix} \sigma_1^2 & & & 0 \\ & \sigma_2^2 & & \\ & & \cdot & \\ & & & \cdot \\ 0 & & & \sigma_K^2 \end{bmatrix}
$$

$$
= \begin{bmatrix} \bar{E}_{r_1} & & & 0 \\ & \bar{E}_{r_2} & & \\ & & \cdot & \\ & & & \cdot \\ 0 & & & \bar{E}_{r_K} \end{bmatrix} \tag{193}
$$

and

$$
\tilde{\boldsymbol{\rho}} = \int_{T_i}^{T_f} \tilde{\mathbf{f}}_I(t)\tilde{\mathbf{f}}_I^\dagger(t)\, dt. \tag{194}
$$

Looking at (192) and (194), we see that all the elements in $\tilde{\boldsymbol{\rho}}$ can be written in terms of time-frequency correlation functions of the signal. The covariance function of the colored noise is

$$
\tilde{K}_c(t, u) = \tilde{\mathbf{f}}_I^T(t)\tilde{\boldsymbol{\Lambda}}\tilde{\mathbf{f}}_I^*(u). \tag{195}
$$

Rewriting (190) in matrix notation gives

$$
\tilde{g}(t) = \tilde{g}_d\tilde{f}(t) + \tilde{\mathbf{g}}^T\tilde{\mathbf{f}}_I(t)
$$

$$
= \tilde{g}_d\tilde{f}(t) + \tilde{\mathbf{f}}_I^T(t)\tilde{\mathbf{g}}, \tag{196}
$$

where

$$
\tilde{\mathbf{g}} \triangleq \begin{bmatrix} \tilde{g}_1 \\ \cdot \\ \cdot \\ \cdot \\ \tilde{g}_K \end{bmatrix}. \tag{197}
$$

Substituting (195) and (196) into (188), we have

$$
\tilde{f}(t) = \int_{-\infty}^{\infty} \{\tilde{\mathbf{f}}_I^T(t)\tilde{\boldsymbol{\Lambda}}\tilde{\mathbf{f}}_I^*(u) + N_0\delta(t - u)\}\{\tilde{g}_d\tilde{f}(u) + \tilde{\mathbf{f}}_I^T(u)\tilde{\mathbf{g}}\}\, du. \tag{198}
$$

This reduces to

$$\tilde{f}(t) = \tilde{g}_d \tilde{\mathbf{f}}_I^T(t) \mathbf{\Lambda} \tilde{\boldsymbol{\rho}}_d + N_0 \tilde{g}_d \tilde{f}(t) + \tilde{\mathbf{f}}_I^T(t) \tilde{\mathbf{\Lambda}} \tilde{\boldsymbol{\rho}}^* \tilde{\mathbf{g}} + N_0 \tilde{\mathbf{f}}_I^T(t) \tilde{\mathbf{g}}, \tag{199}$$

where

$$\tilde{\boldsymbol{\rho}}_d = \int_{-\infty}^{\infty} \tilde{\mathbf{f}}_I^*(u) \tilde{f}(u) \, du. \tag{200}$$

Solving (199), we have

$$\tilde{g}_d = \frac{1}{N_0} \tag{201}$$

and

$$\tilde{\mathbf{g}} = -\frac{1}{N_0^2} \left[\mathbf{I} + \frac{1}{N_0} \tilde{\mathbf{\Lambda}} \tilde{\boldsymbol{\rho}}^* \right]^{-1} \tilde{\mathbf{\Lambda}} \tilde{\boldsymbol{\rho}}_d. \tag{202}$$

This completely specifies the optimum receiver.

Using (196), (201), and (202) in (9.77), we find that the performance is determined by

$$\Delta_o = \frac{\bar{E}_r}{N_0} \left(1 - \frac{1}{N_0} \tilde{\boldsymbol{\rho}}_d^\dagger \left[\mathbf{I} + \frac{1}{N_0} \tilde{\mathbf{\Lambda}} \tilde{\boldsymbol{\rho}}^* \right]^{-1} \tilde{\mathbf{\Lambda}} \tilde{\boldsymbol{\rho}}_d \right). \tag{203}$$

To illustrate these results, we consider a simple example.

Example. Single Interfering Target. In this particular case, the complex envelope of the return from the desired signal is $\sqrt{E_t} \, \tilde{b}_d \tilde{f}(t)$ and the complex envelope of the return from the single interfering target is

$$\tilde{f}_1(t) = \sqrt{E_t} \, \tilde{b}_1 \tilde{f}(t - \tau_1) e^{j\omega_1 t}. \tag{204}$$

Thus, $\tilde{f}_I(t)$, $\tilde{g}$, Λ, ρ, and ρ_d are scalars. Using (202), we obtain

$$\tilde{g}_1 = -\frac{1}{N_0} \left(\frac{2\sigma_1^2}{N_0 + 2\sigma_1^2} \right) \tilde{\rho}_d. \tag{205}$$

observing that

$$\tilde{\rho}_d = \int_{-\infty}^{\infty} \tilde{f}_I^*(u) \tilde{f}(u) \, du = \int_{-\infty}^{\infty} \tilde{f}(u) \tilde{f}^*(u - \tau_1) e^{j\omega_1 u} \, du \tag{206}$$

and

$$\bar{E}_1 = 2E_t \sigma_1^2, \tag{207}$$

we can write the performance expression in (203) as

$$\Delta_o = \frac{\bar{E}_r}{N_0} \left(1 - \frac{\bar{E}_1/N_0}{1 + \bar{E}_1/N_0} \, \theta(\tau_1, \omega_1) \right). \tag{208}$$

The ratio of Δ_o to $\bar{E}_r/N_0$ is plotted in Fig. 10.36. This indicates the degradation in performance due to the interfering target.
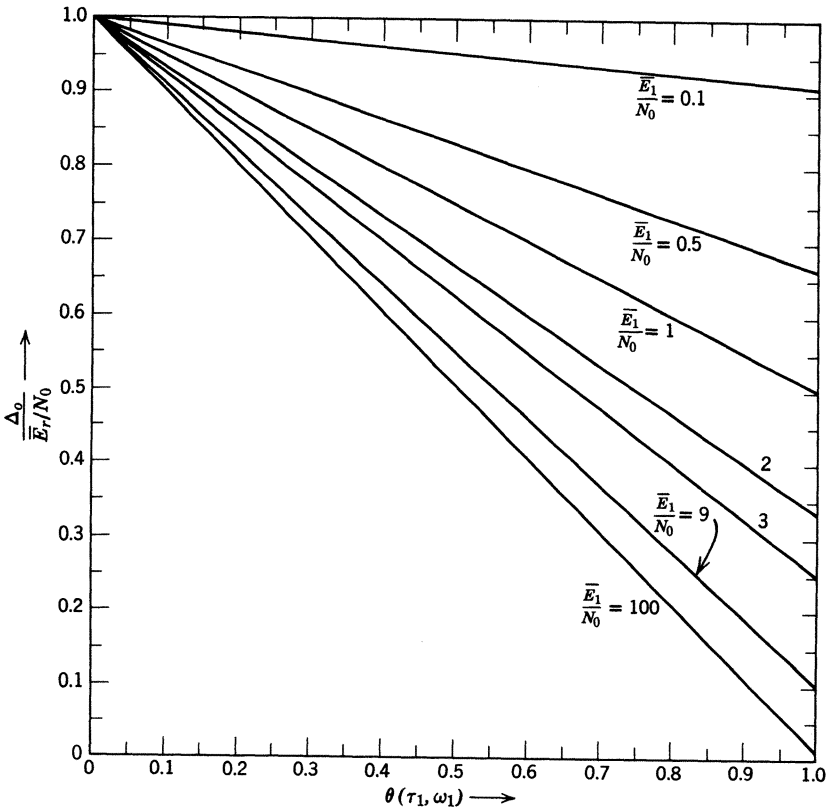
Fig. 10.36 Performance of optimum receiver with single interfering target.

The improvement obtained by using optimum filtering instead of conventional filtering can be found by comparing (208) and (180). The ratio of Δ_o to Δ_{wo} (the performance using a conventional matched filter) is

$$R \triangleq \frac{\Delta_o}{\Delta_{wo}} = \frac{\dfrac{\bar{E}_r}{N_0}\left(1 - \dfrac{\bar{E}_1/N_0}{1 + [\bar{E}_1/N_0]}\,\theta(\tau_1, \omega_1)\right)}{\dfrac{\bar{E}_r}{N_0}\left(1 + \dfrac{\bar{E}_1}{N_0}\,\theta(\tau_1, \omega_1)\right)^{-1}}. \tag{209}$$

This reduces to

$$R = 1 + \frac{(\bar{E}_1/N_0)^2}{(1 + \bar{E}_1/N_0)}\,\theta(\tau_1, \omega_1)[1 - \theta(\tau_1, \omega_1)]. \tag{210}$$

The ratio is plotted in Fig. 10.37 for various values of $\bar{E}_1/N_0$ and $\theta(\tau_1, \omega_1)$. We see that the function is symmetric about $\theta(\tau_1, \omega_1) = 0.5$. The behavior at the endpoints can be explained as follows.

1. As $\theta(\tau_1, \omega_1) \rightarrow 1$, the interference becomes highly correlated with the signal. This means that

$$\tilde{f}_1(t) = \tilde{f}(t - \tau_1)e^{j\omega_1 t} \simeq \tilde{f}(t), \tag{211}$$

so that

$$\tilde{g}(t) = \frac{1}{N_0}\tilde{f}(t) + \tilde{g}_1\tilde{f}_1(t) \simeq \left(\frac{1}{N_0} + \tilde{g}_1\right)\tilde{f}(t). \tag{212}$$

Thus, the optimum and conventional receivers only differ by a gain. Notice that the performance of both receivers become worse as $\theta(\tau_1, \omega_1)$ approaches unity.

2. As $\theta(\tau_1, \omega_1) \rightarrow 0$, the interference becomes essentially uncorrelated with the signal, so that the optimum and conventional receivers are the same. Thus, if we have complete freedom to choose the signal, we design it to make $\theta(\tau_1, \omega_1)$ small and the conventional matched filter will be essentially optimum.
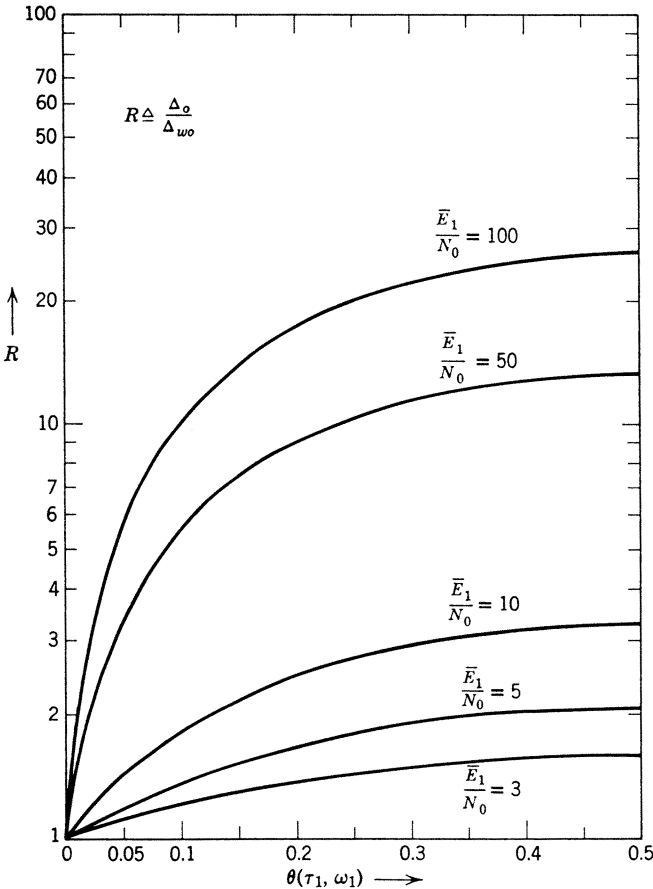

Fig. 10.37   Relative performance of optimum and conventional receivers: single interfering target.

The conclusions of this simple example carry over to the general problem. If possible, we would like to make $\theta(\tau_i, \omega_i)$ zero for all other interfering targets. If we can accomplish this, the optimum and conventional receiver will be the same. When $\theta(\tau_i, \omega_i)$ and E_i/N_0 are large for some values of i, appreciable improvement can be obtained by using the optimum receiver. Notice that our design of the optimum receiver assumes that we know the range and velocity of the interfering targets. In many physical situations this is not a realistic assumption. In these cases we would first have to estimate the parameters of the interfering targets and use these estimates to design the optimum receiver. This procedure is complex, but would be feasible when the interference environment is constant over several target encounters.

This completes our discussion of the discrete resolution problem, and we may now summarize our results.

10.5.4 Summary of Resolution Results

In our study of the discrete resolution problem, we have found that there are two important issues. The first issue is the effect of signal design. Signals that may be very good from the standpoint of accuracy and ambiguity may be very poor in a particular interference environment. Thus, one must match the signal to the expected environment whenever possible.

The second issue is the effect of optimum receiver design. Simple examples indicate that this is fruitful only when the correlation between the interference and the desired signal is moderate. For either small or large correlations, the improvement over conventional matched filtering becomes small. If one can design the signal so that the target return is uncorrelated with the interference, the optimum receiver reduces to the conventional matched filter. In cases when this is not practical, the optimum receiver should be used to improve performances.

We have chosen a particular model of the resolution problem in order to illustrate some of the important issues. Various modifications in the model can be made to accommodate particular physical situations. Two typical problems are the following:

1. The location and number of the interfering targets are not known. We design a receiver that estimates the environment and uses this estimate to detect the target.

2. The targets are known to be located in a certain region (say Ω_I) of the τ, ω plane. The signal is fixed. We design a receiver that reduces the subsidiary peaks (sidelobes) in Ω_I without reducing the value at the correct

target location too much. This problem is usually referred to as the "mismatched filter" or "sidelobe reduction" problem.

A great deal of research has been done on the resolution problem, because it is the critical issue in many radar/sonar systems. There are a number of good references that the interested reader can consult (e.g., [47]-[59]). There is also a great deal of literature on the intersymbol interference problem in digital communication which is of interest (e.g., [61]-[64]).

We have confined our discussion in this section to the discrete resolution problem. After we have developed a model for singly-spread and doubly-spread targets, we shall return to the continuous resolution problem.†

10.6   SUMMARY AND RELATED TOPICS

We first summarize the results that we have obtained, and then discuss some related topics.

10.6.1   Summary

In this section we have studied the problem of estimating the range and velocity of a slowly fluctuating point target. The model of interest is characterized by several features:

1. The signals and random processes of interest are bandlimited around some carrier frequency. This property enabled us to represent the signals and processes either by two real low-pass waveforms or by one complex waveform. Choosing the latter, we reformulated our earlier results in terms of complex quantities. Other than factors of 2 and conjugates in various places, the resulting equations and structures are familiar.

2. The effect of the slowly fluctuating target is to multiply the signal by a complex Gaussian variable. Physically, this corresponds to a random amplitude and phase being introduced into the reflected signal. By assuming that the signal is narrow-band, we can model the effect of the target velocity as a Doppler shift. Thus, the received signal is

$$s(t) = \sqrt{2E_t} \operatorname{Re} [\tilde{b}\tilde{f}(t - \tau)e^{j(\omega_c + \omega)t}]. \tag{213}$$

Using this model, we looked at the problem of estimating range and velocity. The likelihood function led us directly to the optimum receiver.

† The reader who is only interested in the resolution can read pages 459–482 at this point.

In evaluating the performance of the receiver, we encountered the ambiguity function of the signal. Three separate problems were found to be important:

Accuracy. If we can be certain that the error is small (i.e., we are looking at the correct region of the τ, ω plane), the shape of the ambiguity function near the origin completely determines the accuracy. The quantitative accuracy results are obtained by use of the Cramer-Rao inequality.

Ambiguity. The volume-invariance property of the ambiguity function shows that as the volume in the central peak is reduced to improve accuracy, the function has to increase somewhere else in the τ, ω plane. Periodic pulse trains, linear *FM* signals, and pseudo-random sequences were investigated from the standpoint of accuracy and ambiguity.

Resolution. The possible presence of additional interfering targets gives rise to the discrete resolution problem. The principal result of our discussion is the conclusion that the signal should, if possible, be matched to the environment. If we can make the value of the ambiguity function, $\theta(\tau, \omega)$, small at those points in the τ, ω plane where interfering targets are expected, a conventional matched filter receiver is close to optimum.

We now mention some related topics.

10.6.2   Related Topics

Generalized Parameter Sets. We have emphasized the problems of range and Doppler estimation. In many systems, there are other parameters of interest. Typical quantities might be azimuth angle or elevation angle. Because the extension of the results to an arbitrary parameter set is straightforward, we can merely state the results.

We assume that the received signal is $r(t)$, where

$$r(t) = \sqrt{2}\ \text{Re}\ [\{\tilde{b}\sqrt{E_t}\tilde{f}(t, \mathbf{A}) + \tilde{w}(t)\}e^{j\omega_c t}], \qquad -\infty < t < \infty. \quad (214a)$$

Here $\mathbf{A}$ is a nonrandom vector parameter that we want to estimate, and $\tilde{w}(t)$ is a complex white Gaussian process. We also assume

$$\int_{-\infty}^{\infty} |\tilde{f}(t, \mathbf{A})|^2\ dt = 1 \qquad \text{for all } \mathbf{A} \in \chi_{\mathbf{a}}. \quad (214b)$$

The complex function generated by the optimum receiver is

$$\tilde{l}(\mathbf{A}) = \int_{-\infty}^{\infty} \tilde{r}(t)\tilde{f}^*(t, \mathbf{A})\ dt, \quad (215)$$

and the log likelihood function is

$$\ln \Lambda(\mathbf{A}) = \frac{1}{N_0} \frac{\bar{E}_r}{\bar{E}_r + N_0} |\tilde{l}(\mathbf{A})|^2 \qquad (216)$$

[by analogy with (6)]. The function in (216) is calculated as a function of M parameters; $A_1, A_2, \ldots, A_M$. The value of $\mathbf{A}$ where $\ln \Lambda(\mathbf{A})$ has its maximum is $\hat{\mathbf{a}}_{ml}$. Just as on page 277, we investigate the characteristics of $\ln \Lambda(\mathbf{A})$ by assuming that the actual signal is $f(t, \mathbf{A}_a)$. This procedure leads us to a generalized correlation function,

$$\phi(\mathbf{A}, \mathbf{A}_a) \triangleq \int_{-\infty}^{\infty} \tilde{f}(t, \mathbf{A}_a)\tilde{f}^*(t, \mathbf{A}) \, dt, \qquad (217)$$

and a generalized ambiguity function,

$$\theta(\mathbf{A}, \mathbf{A}_a) \triangleq |\phi(\mathbf{A}, \mathbf{A}_a)|^2. \qquad (218)$$

We should also observe that the specific properties derived in Section 10.3 apply only to the time-frequency functions. The problems of accuracy, ambiguity, and resolution in a general parameter space can all be studied in terms of this generalized ambiguity function.

The accuracy formulas follow easily. Specifically, one can show that the elements in the information matrix are

$$J_{ij} = - \frac{\bar{E}_r}{N_0} \left(\frac{\bar{E}_r}{\bar{E}_r + N_0} \right) \left\{ \frac{\partial^2}{\partial A_i \, \partial A_j} \theta(\mathbf{A}, \mathbf{A}_a) \right\}_{\mathbf{A}=\mathbf{A}_a} \qquad (219)$$

Some interesting examples to illustrate these relations are contained in the problems and in *Array Processing* (see [36] also).

Mismatched Filters. There are several cases in which the filters in the receivers are not matched to the signal. One example is estimation in the presence of colored noise. Here the optimum filter is the solution to an integral equation whose kernel is the noise covariance function (e.g., pages 247–251, 329–334). A second example arises when we deliberately mismatch the filter to reduce the sidelobes. The local accuracy performance is no longer optimum, but it may still be satisfactory.

If the filter is matched to $\tilde{g}^*(t)$, the receiver output is

$$\left| \int_{-\infty}^{\infty} \tilde{r}(t)\tilde{g}^*(t) \, dt \right|^2. \qquad (220)$$

By analogy with (17) and (18), we define a time-frequency cross-correlation function,

$$\phi_{fg}(\tau, \omega) \triangleq \int_{-\infty}^{\infty} \tilde{f}\left(t - \frac{\tau}{2}\right) \tilde{g}^*\left(t + \frac{\tau}{2}\right) e^{j\omega t} \, dt, \qquad (221)$$

and a cross-ambiguity function,

$$\theta_{fg}(\tau, \omega) \triangleq |\phi_{fg}(\tau, \omega)|^2. \tag{222}$$

The properties of these functions have been studied by Stutt [37], [44] and Root [38]. (See also Problems 10.6.2–10.6.5 and [68], [74], and [75].)

Detection of a Target with Unknown Parameters. A problem of frequent interest is the detection of targets whose range and velocity are unknown. The model is

$$\tilde{r}(t) = \sqrt{2E_t}\tilde{f}(t - \tau)e^{j\omega t} + \tilde{w}(t), \qquad -\infty < t < \infty : H_1, \tag{223}$$

$$\tilde{r}(t) = \tilde{w}(t), \qquad -\infty < t < \infty : H_0, \tag{224}$$

where τ and ω are unknown nonrandom parameters. Two approaches come to mind.

The first approach is to use a generalized likelihood ratio test (see Section I-2.5). The test is

$$\max_{\tau,\omega} \left\{ \left| \int_{-\infty}^{\infty} \tilde{r}(t)\tilde{f}^*(t - \tau)e^{-j\omega t}\, dt \right|^2 \right\} \underset{H_0}{\overset{H_1}{\gtrless}} \gamma. \tag{225}$$

The threshold γ is adjusted to give the desired P_F. The performance of this test is discussed in detail by Helstrom [39].

The second approach is to divide the region of the τ, ω plane where targets are expected into M rectangular segments (see discussion on pages 302–303 on how to choose the segments). We denote the τ, ω coordinates at the center of the ith cell as τ_i, ω_i. We then consider the binary hypothesis problem

$$\tilde{r}(t) = \sqrt{2E_t}\tilde{f}(t - \tau_i)e^{j\omega_i t} + \tilde{w}(t), \qquad -\infty < t < \infty,$$

$$\text{with probability} \quad p_i = \frac{1}{M}, \qquad i = 1, 2, \ldots, M : H_1 \tag{226}$$

and

$$\tilde{r}(t) = \tilde{w}(t), \qquad -\infty < t < \infty : H_0. \tag{227}$$

This is just the problem of detecting one of M signals that we discussed on page I-405. As we would expect, the performances of the two systems are similar.

Large Time-Bandwidth Signals. In some sonar systems the bandwidth of the signal is large enough that the condition

$$WT \ll \frac{c}{2v} \tag{228}$$

given in (9.23) is not a valid assumption. In these cases we cannot model the time compression as a Doppler shift. Several references [69]–[73] treat this problem, and the interested reader should consult them.

This completes our discussion of slowly fluctuating targets and channels. We now consider the next level of target in our hierarchy.

10.7   PROBLEMS

P.10.1   Receiver Derivation and Signal Design

Problem 10.1.1. The random variable $\tilde{n}(\tau, \omega)$ is defined in (13). Prove that the probability density of $\tilde{n}(\tau, \omega)$ is not a function of τ and ω.

Problem 10.1.2. Consider the Gaussian pulse with linear FM in (44a).

1. Verify the results in (46)–(48) directly from the definitions in the Appendix.

2. Verify the results in (46)–(48) by using (96)–(98).

Problem 10.1.3. Let

$$\tilde{f}(t) = c \sin^2\left(\frac{2\pi t}{T}\right), \qquad 0 \leq t \leq T,$$

where c is a normalizing constant. Find $\theta(\tau, \omega)$.

Problem 10.1.4. Let

$$\tilde{f}(t) = \tilde{f}_1(t) + \tilde{f}_2(t),$$

where

$$\tilde{f}_1(t) = \begin{cases} \dfrac{1}{\sqrt{T_1}}, & 0 \leq t \leq T_1, \\ 0, & \text{elsewhere,} \end{cases}$$

and

$$\tilde{f}_2(t) = \begin{cases} \dfrac{1}{\sqrt{T_2}}\, e^{-j\omega_2 t}, & T_p \leq t \leq T_p + T_2, \\ 0, & \text{elsewhere.} \end{cases}$$

Assume that

$$T_p > T_1.$$

1. Find $\theta(\tau, \omega)$.

2. Plot for the case

$$T_1 \ll T_2,$$

$$\frac{\omega_2}{2\pi} \gg \frac{1}{T_1}.$$

P.10.2   Performance Analysis

Problem 10.2.1. Derive the expressions for J_{12} and J_{22} that are given in (64) and (65).

Problem 10.2.2. Derive the expressions in (96)–(98).

Problem 10.2.3. Consider the expression in (6). Expand $\tilde{L}(\tau, \omega)$ in a power series in τ and ω around the point

$$\tau = \hat{\tau}_{ml},$$

$$\omega = \hat{\omega}_{ml}.$$

Assuming that the errors are small, find an expression for their variance.

P.10.3   Properties of $\phi(\tau, \omega)$ and $\theta(\tau, \omega)$

Problem 10.3.1. In Property 5 we derived an alternative representation of $\phi(\tau, \omega)$. Prove that another alternative representation is

$$\phi(\tau, \omega) = \frac{e^{-j\omega\tau/2}}{2\pi} \iint\limits_{-\infty}^{\infty} \tilde{f}\left(\beta - \frac{\tau}{2}\right) \tilde{F}^*(j\omega - j\alpha) e^{j\alpha\beta + j\alpha\tau/2} \, d\alpha \, d\beta.$$

Problem 10.3.2. The transmitted waveform, $\tilde{f}(t)$, has a Fourier transform,

$$\tilde{F}\{f\} = \begin{cases} \dfrac{1}{\sqrt{W}}, & |f| \leq W, \\ 0, & |f| > W. \end{cases}$$

Find $\phi\{\tau, f\}$.

Problem 10.3.3. The transmitted waveform, $\tilde{f}(t)$, has a Fourier transform which can be written as

$$\tilde{F}\{f\} = c \sum_{k=-n}^{k=n} \tilde{U}\{f - kW_s\},$$

where

$$\tilde{U}\{f\} = \begin{cases} \dfrac{1}{\sqrt{W}}, & |f| \leq W, \\ 0, & |f| > W, \end{cases}$$

$$W_s \gg W,$$

and c is a normalizing factor.

1. Find $\phi\{\tau, f\}$.
2. How would you synthesize $\tilde{f}(t)$?

Problem 10.3.4. Partial Volume Invariances. Prove

$$\int_{-\infty}^{\infty} |\tilde{F}\{x\}|^2 |\tilde{F}\{x + f\}|^2 \, dx = \int_{-\infty}^{\infty} \theta\{\tau, f\} \, df.$$

Notice that this is a partial volume invariance property. The total volume in a strip of width $\Delta\tau$ at some value of τ cannot be altered by phase modulation of the waveform.

Problem 10.3.5.

1. Prove

$$\int_{-\infty}^{\infty} |\tilde{f}(t)|^2 |\tilde{f}(t+\tau)|^2 \, dt = \int_{-\infty}^{\infty} \theta\{\tau,f\} \, d\tau \qquad (P.1)$$

directly from the definition.

2. Prove the relationship in (P.1) by inspection by using the result of Problem 10.3.4 and the duality principle.

Note: This is another partial volume invariance property.

Problem 10.3.6.

1. Expand the ambiguity function, $\theta\{\tau,f\}$, in a Taylor series around the origin.

2. Express the coefficients of the quadratic terms as functions of $\overline{t^2}$, $\overline{\omega t}$, and $\overline{\omega^2}$.

Problem 10.3.7 [40]. Derive the following generalization of Property 9. Assume

$$\begin{vmatrix} c_{11} & c_{12} \\ c_{21} & c_{22} \end{vmatrix} = \pm 1$$

and

$$\phi_1\{\tau,f\} \sim \tilde{f}_1(t).$$

If

$$\tilde{f}_2(t) = |c_{11}|^{1/2} \int_{-\infty}^{\infty} df \exp\left[j2\pi c_{11} f\left(t - \frac{c_{12}}{2}f\right) \right]$$

$$\times \int_{-\infty}^{\infty} \tilde{f}_1(z) \exp\left[-j2\pi z\left(f - \frac{c_{21}}{2c_{11}}z\right) \right] dz,$$

then

$$|\phi_2\{\tau,f\}| = |\phi_1\{c_{11}\tau + c_{12}f, -c_{21}\tau - c_{22}f\}|.$$

Problem 10.3.8 [12]. Derive the following "volume" invariance property:

$$\iint\limits_{-\infty}^{\infty} \theta\{\tau,f\}^p \, d\tau \, df \le \frac{1}{p}\, \theta\{\tau,f\},$$

where p is an integer greater than or equal to 1.

Problem 10.3.9 [41]–[43]. Assume that we expand $\tilde{f}(t)$ using a CON set,

$$\tilde{f}(t) = \sum_{i=1}^{\infty} f_i \tilde{u}_i(t), \qquad -\infty < t < \infty.$$

Let

$$\phi_{ik}\{\tau,f\} \triangleq \int_{-\infty}^{\infty} \tilde{u}_i\left(t - \frac{\tau}{2}\right) \tilde{u}_k^*\left(t + \frac{\tau}{2}\right) e^{j2\pi ft} \, dt$$

denote the time-frequency cross-correlation function of $\tilde{u}_i(t)$ and $\tilde{u}_k(t)$.

1. Prove

$$\int\!\!\!\int\limits_{-\infty}^{\infty} \phi_{ik}\{\tau, f\}\phi_{mn}^*\{\tau, f\}\, d\tau\, df = \delta_{kn}\,\delta_{im}.$$

2. Compare this result with Property 3.
3. Prove

$$\phi_{\tilde{f}}\{\tau, f\} = \sum_{i=1}^{\infty}\sum_{k=1}^{\infty} f_i f_k^* \phi_{ik}\{\tau, f\}$$

and

$$c_{ik} \triangleq f_i f_k^* = \int\!\!\!\int\limits_{-\infty}^{\infty} \phi_{\tilde{f}}\{\tau, f\}\phi_{ik}^*\{\tau, f\}\, d\tau\, df.$$

Problem 10.3.10. The Hermite waveforms are

$$\tilde{f}_n(t) = \frac{2^{1/4}}{\sqrt{n!}}\, e^{-\pi t^2} H_n(2\sqrt{\pi}\,t), \qquad -\infty < t < \infty, \quad n = 1, 2, \ldots, \qquad \text{(P.1)}$$

where $H_n(t)$ is the nth-order Hermite polynomial,

$$H_n(t) = (-1)^n e^{t^2/2}\frac{d^n}{dt^n}\, e^{-t^2/2}, \qquad -\infty < t < \infty. \qquad \text{(P.2)}$$

1. Find $\tilde{F}\{f\}$.
2. Prove that

$$\phi_n\{\tau, f\} = \exp\left[-\frac{\pi}{2}(\tau^2 + f^2)\right]L_n[\pi(\tau^2 + \phi^2)], \qquad \text{(P.3)}$$

where $L_n(x)$ is the nth-order Laguerre polynomial

$$L_n(x) = \begin{cases} \dfrac{1}{n!}\, e^x \dfrac{d^n}{dx^n}\, (x^n e^{-x}), & x \geq 0, \\ 0, & x < 0. \end{cases}$$

3. Verify that your answer reduces to Fig. 10.8 for $n = 1$.
Comment: Plots of these waveforms are given in [46].
4. Notice that the time-frequency autocorrelation function is rotationally symmetric.
   a. Use this fact to derive $\tilde{F}\{f\}$ by inspection (except for a phase factor).
   b. What does Property 9 imply with respect to the Hermite waveforms?

Problem 10.3.11 [14]. Let

$$\tilde{f}(t) = \begin{cases} \sqrt{\dfrac{1}{T}}\exp\left[j\,\Delta\theta \sin\dfrac{2\pi t}{T}\right], & |t| < \dfrac{T}{2}, \\ 0, & \text{elsewhere.} \end{cases}$$

1. Find $\tilde{F}\{f\}$.
2. Find $|\phi\{\tau, f\}|$.

Problem 10.3.12 [14]. Let

$$\tilde{f}(t) = \left(\frac{2k^2}{\pi}\right)^{1/4} e^{-(k^2-jct)t^2}, \qquad -\infty < t < \infty.$$

This is a pulse with a Gaussian envelope and parabolic frequency modulation.
  Find $|\phi\{\tau, f\}|$.

Problem 10.3.13. A waveform that is useful for analytic purposes is obtained from the $\tilde{f}(t)$ in (32) by letting

$$T \to 0$$

and

$$n \to \infty.$$

while holding nT constant.
We denote the resulting signal as $i_\delta(t)$.

  1. Plot $|\phi\{\tau, f\}|$ for this limiting case. Discuss suitable normalizations.

  2. Define

$$\tilde{f}(t) = \int_{-\infty}^{\infty} \tilde{h}(\tau) i_\delta(t - \tau) \, d\tau.$$

Express $\phi_{\tilde{f}}\{\tau, f\}$ in terms of $\phi_{i_\delta}\{\tau, f\}$.

Problem 10.3.14. Consider the problem in which we transmit two disjoint pulses, $\tilde{f}_1(t)$ and $\tilde{f}_2(t)$. The complex envelope of received waveform on H_1 is

$$\tilde{r}(t) = \sqrt{E_1}\,\tilde{b}_1\tilde{f}_1(t - \tau)e^{j\omega t} + \sqrt{E_2}\,\tilde{b}_2\tilde{f}_2(t - \tau)e^{j\omega t} + \tilde{w}(t), \quad -\infty < t < \infty : H_1$$

The multipliers $\tilde{b}_1$ and $\tilde{b}_2$ are statistically independent, zero-mean complex Gaussian random variables,

$$E[|\tilde{b}_i|^2] = 2\sigma_b{}^2.$$

On H_0, only $\tilde{w}(t)$ is present,

  1. Find the likelihood function and the optimum receiver.

  2. How is the signal component at the output of the optimum receiver related to $\phi_1\{\tau, f\}$ and $\phi_2\{\tau, f\}$?

Problem 10.3.15. Consider a special case of Problem 10.3.14 in which $\tilde{f}_1(t)$ is a short rectangular pulse and $\tilde{f}_2(t)$ is a long rectangular pulse.

  1. Sketch the signal component at the output of the optimum receiver.

  2. Discuss other receiver realizations that might improve the global accuracy. For example, consider a receiver whose signal output consists of $\theta_1\{\tau, f\}$ times $\theta_2\{\tau, f\}$.

P.10.4   Coded Pulse Sequences

Problem 10.4.1. Consider the periodic pulse sequence in Fig. 10.21. Assume that

$$\omega_n = (n - 1)\omega_\Delta,$$

where

$$\frac{\omega_\Delta}{2\pi} = \frac{1}{T_s}.$$

1. Find $|\phi(\tau, \omega)|$.
2. Plot the result in part 1.

Problem 10.4.2. Consider the signal in (145). Assume that

$$a_1 = 1,$$

$$a_n = 1, \quad \text{with probability } \tfrac{1}{3}, \text{ for } n = 2, \ldots, 7,$$

$$a_n = 0, \quad \text{with probability } \tfrac{2}{3}, \text{ for } n = 2, \ldots, 7,$$

$$a_8 = 1.$$

1. Find $E\{|\phi(\tau, \omega)|\}$.
2. Discuss the sidelobe behavior in comparison with a periodic pulse train.
3. How would you use these results to design a practical signal?

Problem 10.4.3. Consider the three-stage shift register in Fig. 10.26. Compute $\phi\{\tau, \omega\}$ for various initial states of the shift register. Assume that the output consists of one period.

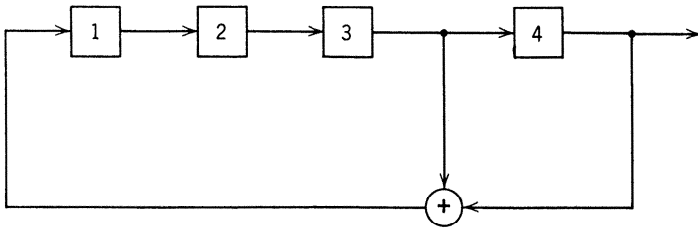**Problem 10.4.4.** Consider the shift register system is Fig. P.10.1.

Fig. P.10.1

1. Verify that this feedback connection gives a maximum length sequence. We use the notation [4, 3] to indicate that the outputs of stages 3 and 4 are fedback.

2. Does the shift register with connections [4, 2] generate a maximum length sequence?

Problem 10.4.5.

1. Consider a shift register with connections [5, 3]. Verify that it generates a maximal length sequence.

2. Does the shift register with connections [5, 4, 3, 2] generate a maximal length sequence?

3. Does the shift register with connections [5, 4, 3, 1] generate a maximal length sequence?

Problem 10.4.6. Verify that shift registers with connections [6, 5], [6, 5, 4, 1], and [6, 5, 3, 2] generate maximal length sequences.

P.10.5   Resolution

Problem 10.5.1. Consider the following three hypothesis problem.

$$\tilde{r}(t) = \sqrt{E_1}\,\tilde{b}_1\tilde{f}(t - \tau_1)e^{j\omega_1 t} + \sqrt{E_2}\,\tilde{b}_2\tilde{f}(t - \tau_2)e^{j\omega_2 t} + \tilde{w}(t), \qquad -\infty < t < \infty : H_2,$$

$$\tilde{r}(t) = \sqrt{E_1}\tilde{b}_1\tilde{f}(t = \tau_1)e^{j\omega_1 t} + \tilde{w}(t), \qquad\qquad\qquad -\infty < t < \infty : H_1,$$

$$\tilde{r}(t) = \tilde{w}(t), \qquad\qquad\qquad\qquad\qquad\qquad\qquad -\infty < t < \infty : H_0.$$

The multipliers $\tilde{b}_1$ and $\tilde{b}_2$ are zero-mean complex Gaussian random variables with mean-square values $2\sigma_1^2$ and $2\sigma_2^2$. The parameters τ_1, τ_2, ω_1, and ω_2 are assumed known. The additive noise is a complex white Gaussian process with spectral height N_0.

Find the optimum Bayes test. Leave the costs as parameters.

Problem 10.5.2. Consider the same model as in Problem 10.5.1. We design a test using the MAP estimates of $|\tilde{b}_1|$ and $|\tilde{b}_2|$.

1. Find $|\widehat{\tilde{b}_1}|$, given that H_1 is true. Find $|\widehat{\tilde{b}_1}|$ and $|\widehat{\tilde{b}_2}|$, given that H_2 is true.

2. Design a test based on the above estimates. Compare it with the Bayes test in Problem 10.5.1.

3. Define P_F as

$$P_F = \Pr\,[\text{say } H_1 \text{ or } H_2 \mid H_0].$$

Find P_{D_1} and P_{D_2}.

Problem 10.5.3. Assume that a rectangle in the τ, ω plane with dimension $T_* \times \Omega_*$ is of interest. We use a grid so that there are M cells of interest (see discussion on pages 302–303). In each cell there is at most one target. We want to estimate the number of targets that are present and the cells which they occupy.

Discuss various procedures for implementing this test. Consider both performance and complexity.

Problem 10.5.4. An alternative way to approach the optimum receiver problem in Section 10.5.3 is to find the eigenfunctions and eigenvalues of the interfering noise process. From (195),

$$\tilde{K}_c(t, u) = \tilde{\mathbf{f}}_I{}^T(t)\tilde{\boldsymbol{\Lambda}}\,\tilde{\mathbf{f}}_I{}^*(u), \qquad -\infty < t, u < \infty.$$

We want to write

$$\tilde{K}_c(t, u) = \sum_{i=1}^{\infty} \tilde{\lambda}_i\tilde{\phi}_i(t)\tilde{\phi}_i{}^*(u), \qquad -\infty < t, u < \infty.$$

1. Find $\tilde{\lambda}_i$ and $\tilde{\phi}_i(t)$. How many eigenvalues are nonzero?

2. Use the result in part 1 to find the optimum receiver.

3. Find Δ_o.

Problem 10.5.5. We want to communicate over the resolvable multipath channel shown in Fig. P.10.2. To investigate the channel structure, we transmit a *known* sounding signal with complex envelope $\tilde{f}(t)$. The complex envelope of the received waveform is

$$\tilde{r}(t) = \sum_{i=1}^{3} \sqrt{2}\,\tilde{b}_i\tilde{f}(t - \tau_i) + \tilde{w}(t),$$
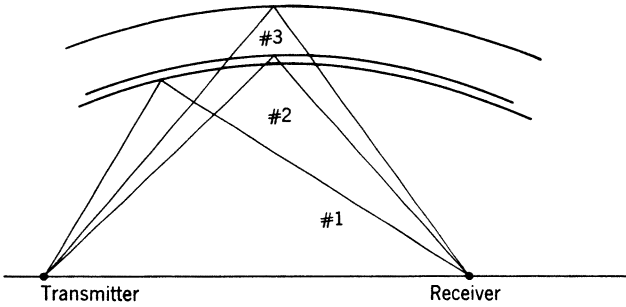
Fig. P.10.2

where the $\tilde{b}_i$ are independent zero-mean complex Gaussian variables with variances $2\sigma_i^2$ and $\tilde{w}(t)$ is a zero-mean complex Gaussian process with spectral height N_0. The signal outputs of the three channels are disjoint in time. The τ_i are modeled as independent, uniformly distributed, random variables, $U[-T, T]$, where T is large.

Derive the optimum receiver for estimating $\hat{\tau}_{i,\text{map}}$.

Problem 10.5.6. Consider the following detection problem:

$$\tilde{r}(t) = \sqrt{2E_t}\,\tilde{b}\tilde{f}(t) + \tilde{w}(t), \qquad T_i \leq t \leq T_f : H_1,$$

$$\tilde{r}(t) = \tilde{w}(t), \qquad\qquad\quad T_i \leq t \leq T_f : H_0.$$

The deterministic signal $\tilde{f}(t)$ has unit energy and is zero outside the interval $(0, T)$. [This interval is included in (T_i, T_f).] The multiplier $\tilde{b}$ is a zero-mean complex Gaussian random variable,

$$E\{|\tilde{b}|^2\} = 2\sigma_b^2.$$

The additive noise, $\tilde{w}(t)$, is a complex zero-mean Gaussian process with spectral height N_0.

1. Find the optimum detector. Compute Δ_o, P_D, and P_F.
2. Now assume that the received signal on H_1 is actually

$$\tilde{r}(t) = \sqrt{2E_t}\,\tilde{b}\tilde{f}(t - \tau)e^{j\omega t} + \tilde{w}(t), \qquad T_i \leq t \leq T_f : H_1,$$

where τ and ω are small. We process $\tilde{r}(t)$ using the detector in part 1. Compute the change in Δ as a function of τ and ω. Express your answer in terms of $\theta(\tau, \omega)$, the ambiguity function of $\tilde{f}(t)$.

3. Design several signals that are insensitive to small changes in τ and ω. Explain your design procedure.

Problem 10.5.7. Consider the resolution problem described in (173)–(180). A conventional receiver is used. The degradation in performance is given by

$$\Delta_I = \sum_{i=1}^{K} \frac{\bar{E}_{r_i}}{N_0}\,\theta(\tau_i, \omega_i).$$

Assume that the interfering targets all have zero Doppler relative to the desired target and that $\bar{E}_{r_i} = \bar{E}_I$. Then

$$\Delta_I = \frac{\bar{E}_I}{N_0} \sum_{i=1}^{K} \theta(\tau_i, 0).$$

Now assume that the targets are uniformly spaced on th: τ-axis such that there is a target in each successive $\Delta\tau$ interval. Defining

$$\bar{E}_I = A \, \Delta\tau$$

and letting $K \to \infty$ and $\Delta\tau \to 0$, we obtain the integral

$$\Delta_I = \frac{A}{N_0} \int_{-\infty}^{\infty} \theta(\tau, 0) \, d\tau = \frac{A}{N_0} \Delta_R.$$

Comment: The resolution constant Δ_R was first introduced by Woodward [60].

Prove that

$$\Delta_R = \int_{-\infty}^{\infty} |F\{f\}|^4 \, df.$$

Notice that the signal $\tilde{f}(t)$ is always normalized.

Problem 10.5.8. Extend the ideas of Problem 10.5.7 to find a Doppler resolution constant

$$\Delta_D \triangleq \int_{-\infty}^{\infty} \theta\{0, f\} \, df.$$

Prove that

$$\Delta_D = \int_{-\infty}^{\infty} |\tilde{f}(t)|^4 \, dt.$$

Problem 10.5.9. Compute Δ_R, Δ_D, and $\Delta_R\Delta_D$ for the following:

1. A simple Gaussian pulse (25).
2. A rectangular pulse.

Problem 10.5.10 [39, Chapter X]. Consider the following resolution problem. The received waveforms on the four hypotheses are

$$
\begin{aligned}
r(t) &= w(t), & 0 \le t \le T : H_0, \\
r(t) &= Af(t) + w(t), & 0 \le t \le T : H_1, \\
r(t) &= Bg(t) + w(t), & 0 \le t \le T : H_2, \\
r(t) &= Af(t) + Bg(t) + w(t), & 0 \le t \le T : H_3.
\end{aligned}
$$

The multipliers A and B are unknown nonrandom variables. The signals $f(t)$ and $g(t)$ are known waveforms with unit energy, and

$$\int_0^T f(t)g(t) \, dt = \rho.$$

The additive noise $w(t)$ is a sample function of a white Gaussian random process with spectral height $N_0/2$. (Notice that the waveforms are not bandpass.) We want to derive a generalized likelihood ratio test (see Section I-2.5).

1. Assume that H_3 is true. Prove that

$$\hat{a}_{ml} = \frac{1}{1-\rho^2} \int_0^T [f(t) - \rho g(t)] r(t)\, dt.$$

2. Find $\hat{b}_{ml}$.

3. Calculate $E[\hat{a}_{ml}]$, $E[\hat{b}_{ml}]$, Var $[\hat{a}_{ml}]$, Var $[\hat{b}_{ml}]$, and Cov $[\hat{a}_{ml}, \hat{b}_{ml}]$ under the four hypotheses.

4. Assume that we use the test

$$\hat{a}_{ml} \underset{H_0 \text{ or } H_2}{\overset{H_1 \text{ or } H_3}{\gtrless}} \gamma_a,$$

$$\hat{b}_{ml} \underset{H_0 \text{ or } H_1}{\overset{H_2 \text{ or } H_3}{\gtrless}} \gamma_b.$$

Calculate P_{Fa}, P_{Da}, P_{Fb}, and P_{Db}. Verify that both P_{Da} and P_{Db} decrease monotonically as ρ increases.

Problem 10.5.11 [39, Chapter X]. Consider the bandpass version of the model in Problem 10.5.10. Assume that the complex envelopes on the four hypotheses are

$$\tilde{r}(t) = \tilde{w}(t), \qquad\qquad\qquad\qquad 0 \le t \le T : H_0,$$
$$\tilde{r}(t) = Ae^{j\varphi_a}\tilde{f}(t) + \tilde{w}(t), \qquad\qquad 0 \le t \le T : H_1,$$
$$\tilde{r}(t) = Be^{j\varphi_b}\tilde{g}(t) + \tilde{w}(t), \qquad\qquad 0 \le t \le T : H_2,$$
$$\tilde{r}(t) = Ae^{j\varphi_a}\tilde{f}(t) + Be^{j\varphi_b}\tilde{g}(t) + \tilde{w}(t), \quad 0 \le t \le T : H_3.$$

The multipliers A and B are unknown nonrandom variables. The phases φ_a and φ_b are statistically independent, uniformly distributed random variables on $(0, 2\pi)$. The complex envelopes $\tilde{f}(t)$ and $\tilde{g}(t)$ are known unit energy signals with

$$\int_{-\infty}^{\infty} \tilde{f}(t)\tilde{g}^*(t)\, dt = \tilde{\rho}_{fg}.$$

The additive noise $\tilde{w}(t)$ is a sample function of a complex white Gaussian process with spectral height N_0.

1. Find $\hat{a}_{ml}$ and $\hat{b}_{ml}$ under the assumption that H_3 is true.

2. Calculate $E[\hat{a}_{ml}]$, $E[\hat{b}_{ml}]$, Var $[\hat{a}_{ml}]$, Var $[\hat{b}_{ml}]$, and Cov $[\hat{a}_{ml}, \hat{b}_{ml}]$ under the four hypotheses.

3. The test in part 4 of Problem 10.5.10 is used. Calculate the performance.

Problem 10.5.12 [39, Chapter X]. The model in Problem 10.5.11 can be extended to include an unknown arrival time. The complex envelope of the received waveform on H_3 is

$$\tilde{r}(t) = Ae^{j\varphi_a}\tilde{f}(t - \tau) + Be^{j\varphi_b}\tilde{g}(t - \tau) + \tilde{w}(t), \quad -\infty < t < \infty : H_3.$$

The other hypotheses are modified accordingly.

1. Find a receiver that generates $\hat{a}_{ml}$, $\hat{b}_{ml}$, and $\hat{\tau}_{ml}$.

2. Find the corresponding likelihood ratio test.

Problem 10.5.13. Consider the following model of the resolution problem. The complex envelopes of the received waveforms on the two hypotheses are

$$\tilde{r}(t) = \tilde{b}_d \tilde{f}(t) + \sum_{i=1}^{N} B_i e^{j\varphi_i} \tilde{f}(t - \tau_i) e^{j\omega_i t} + \tilde{w}(t); \qquad -\infty < t < \infty : H_1,$$

$$\tilde{r}(t) = \sum_{i=1}^{N} B_i e^{j\varphi_i} \tilde{f}(t - \tau_i) e^{j\omega_i t} + \tilde{w}(t), \qquad -\infty < t < \infty : H_0.$$

The model is the same as that in Section 10.5.3 (page 329) except that the B_i are assumed to be *unknown, nonrandom* variables. The φ_i are statistically independent, uniformly distributed random variables. The τ_i and ω_i are assumed known.

1. Find the generalized likelihood ratio test for this model. (*Hint:* Review Section I-2.5.)

2. Evaluate P_F and P_D.

Comment: This problem is similar to that solved in [59].

P.10.6 Summary and Related Topics

Problem 10.6.1. Generalized Likelihood Ratio Tests. Consider the following composite hypothesis problem

$$\tilde{r}(t) = \sqrt{2E_t} \, \tilde{b} \tilde{f}(t - \tau) e^{j\omega t} + \tilde{w}(t), \qquad -\infty < t < \infty : H_1,$$

$$\tilde{r}(t) = \tilde{w}(t), \qquad\qquad -\infty < t < \infty : H_0.$$

The multiplier $\tilde{b}$ is a zero-mean complex Gaussian variable,

$$E\{|\tilde{b}|^2\} = 2\sigma_b^2,$$

and $\tilde{w}(t)$ is a complex zero-mean Gaussian white noise process with spectral height N_0. The quantities τ and ω are *unknown nonrandom* variables whose ranges are known:

$$\tau_0 < \tau \le \tau_1,$$

$$\omega_0 < \omega \le \omega_1.$$

Find the generalized likelihood ratio test and draw a block diagram of the optimum receiver.

Problem 10.6.2. The time-frequency cross-correlation function is defined by (221) as

$$\phi_{fg}\{\tau, f\} = \int_{-\infty}^{\infty} \tilde{f}\left(t - \frac{\tau}{2}\right) \tilde{g}^*\left(t + \frac{\tau}{2}\right) e^{j2\pi ft} \, dt.$$

In addition,

$$\theta_{fg}\{\tau, f\} \triangleq |\phi_{fg}\{\tau, f\}|^2.$$

Assume that

$$\int_{-\infty}^{\infty} |\tilde{f}(t)|^2 \, dt = \int_{-\infty}^{\infty} |\tilde{g}(t)|^2 \, dt = 1.$$

1. Prove

$$\iint_{-\infty}^{\infty} \theta_{fg}\{\tau, f\} \, d\tau \, df = 1.$$

2. Does $\theta_{fg}\{0, 0\}$ always equal unity? Justify your answer.

3. Is the equality

$$\theta_{fg}\{\tau, f\} \leq \theta_{fg}\{0, 0\}$$

true? Justify your answer.

Problem 10.6.3 [44]. As in (221), we define the time-frequency cross-correlation function as

$$\phi_{fg}\{\tau, f\} = \int_{-\infty}^{\infty} \tilde{f}\left(t - \frac{\tau}{2}\right)\tilde{g}^*\left(t + \frac{\tau}{2}\right)e^{j2\pi ft}\,dt.$$

Verify the following properties.

1.
$$\phi_{fg}\{\tau, f\} = \int_{-\infty}^{\infty} \tilde{G}^*\left(x + \frac{f}{2}\right)\tilde{F}\left(x - \frac{f}{2}\right)e^{j2\pi f\tau}\,dx.$$

2.
$$\phi_{fg}\{\tau, f\} = \int_{-\infty}^{\infty} \tilde{F}(x)\tilde{G}^*\{y\}\exp\left[j2\pi\left(\frac{\tau f}{2} - xy - fx + \tau y\right)\right]\,dx\,dy.$$

3.
$$\phi_{fg}\{\tau, f\} = \phi_{gf}\{-\tau, -f\}.$$

4.
$$\theta_{fg}\{\tau, f\} = \theta_{gf}\{-\tau, -f\}.$$

Problem 10.6.4 [44]. Prove

$$\iint\limits_{-\infty}^{\infty} \phi_{12}\{\tau, f\}\phi_{34}^*\{\tau, f\}e^{j2\pi[fx - \tau y]}\,d\tau\,df = \phi_{13}\{x, y\}\phi_{24}^*\{x, y\}.$$

Problem 10.6.5 [44]. Prove

$$\iint\limits_{-\infty}^{\infty} \theta_{fg}\{\tau, f\}e^{j2\pi(fx - \tau y)}\,d\tau\,df = \phi_f(x, y)\phi_g^*(x, y).$$

Problem 10.6.6. Consider the following estimation problem. The complex envelope of the received signal is

$$\tilde{r}(t) = \sqrt{E_t}\,\tilde{f}(t - \tau)e^{j\omega t} + \tilde{n}_c(t) + \tilde{w}(t), \qquad -\infty < t < \infty.$$

The colored Gaussian noise has a spectrum

$$S_{n_c}(\omega) = \frac{2\alpha P_c}{\omega^2 + \alpha^2}.$$

The complex white noise has spectral height N_0.

1. Find the optimum filter for estimating τ and ω. Express it as a set of paths consisting of a cascade of a realizable whitening filter, a matched filter, and a square-law envelope detector.

2. Write an expression for the appropriate ambiguity function at the output of the square-law envelope detector. Denote this function as $\theta_{fw}(\tau, \omega)$.

3. Denote the impulse response of the whitening filter as $\tilde{h}_{wr}(u)$. Express the ambiguity function $\theta_{fw}(\tau, \omega)$ in terms of $\phi_f(\tau, \omega)$, $\theta_f(\tau, \omega)$, and $\tilde{h}_{wr}(u)$. (Recall Property 11 on page 311.)

Problem 10.6.7 (continuation).

1. Derive an expression for the elements in the information matrix **J** [see (63)–(65)]. These formulas give us a bound on the accuracy in estimating τ and ω.

2. Is your answer a function of the actual value of τ or the actual value of ω? Is your result intuitively logical?

Problem 10.6.8. Consider the special case of Problem 10.6.6 in which

$$N_0 = 0$$

and

$$\tilde{f}(t) = \begin{cases} c \sin^2\left(\dfrac{2\pi}{T} t\right), & 0 \leq t \leq T, \\ 0, & \text{elsewhere.} \end{cases}$$

Evaluate $\theta_{fw}(\tau, \omega)$.

Problem 10.6.9. Generalize the results of Problem 10.6.6 so that they include a colored noise with an arbitrary rational spectrum.

Problem 10.6.10. Consider the model in (214a), but do not impose the constraint in (214b).

1. Find the log likelihood function.

2. Evaluate the Cramér-Rao bound.

Problem 10.6.11. In this problem we consider the simultaneous estimation of range, velocity, and acceleration.

Assume that the complex envelope of the received waveform is

$$\tilde{r}(t) = \sqrt{E_t}\, \breve{b} \sqrt{1 - \dot{\tau}(t)}\, \tilde{f}(t - \tau(t)) e^{-j2\omega f_c \tau(t)} + \tilde{w}(t), \quad -\infty < t < \infty,$$

where

$$\tau(t) \triangleq \tau + \frac{v}{f_c} t + \frac{\alpha}{2f_c} t^2.$$

The parameter τ, v, and α are unknown nonrandom parameters.

1. Find $\hat{\tau}_{ml}$, $\hat{v}_{ml}$, and $\hat{\alpha}_{ml}$.

2. Compute the Cramér-Rao bound.

See [65] or [66] for a complete discussion of this problem.

REFERENCES

[1] J. Ville, "Theorie et application de la notion de signal analytique," Cables et Transmission **2**, No. 1, 61–74 (1948).

[2] S. J. Mason and H. J. Zimmerman, *Electronic Circuits, Signals, and Systems*, Wiley, New York, 1960, p. 367.

[3] R. H. Dicke, U.S. Patent, 2,624,876, September 14, 1945.

[4] S. Darlington, U.S. Patent 2,678,997, December 31, 1949.

[5] E. Huttman, German Patent 768,068, March 22, 1940.

[6] W. A. Cauer, German Federal Republic Patent 892,774.

[7] C. E. Cooke, "Pulse Compression—Key to More Efficient Radar Transmission," Proc. IRE **48**, 310–316 (1960).

[8] P. M. Woodward and I. L. Davies, "A Theory of Radar Information," Phil. Mag. **41**, 1001–1017 (1950).

[9] W. M. Siebert, "A Radar Detection Philosophy," IRE Trans. Information Theory **IT-2**, 204–221 (Sept. 1956).

[10] W. M. Siebert, "Studies of Woodward's Uncertainty Function," Research Laboratory of Electronics, Massachusetts Institute of Technology, Cambridge, Mass., Quarterly Progress Report, April 1958, pp. 90–94.

[11] R. M. Lerner, "Signals with Uniform Ambiguity Functions," 1958 IRE Trans. Natl. Conv. Rec., Pt. 4, pp. 27–36.

[12] R. Price and E. M. Hofstetter, "Bounds on the Volume and Height Distributions of the Ambiguity Function," IEEE Trans. Information Theory **IT-11**, 207–214 (1965).

[13] A. W. Rihaczek, "Radar Resolution Properties of Pulse Trains," Proc. IEEE **52**, 153–164 (1964).

[14] C. E. Cook and M. Bernfeld, *Radar Signals: An Introduction to Theory and Application*, Academic Press, New York, 1967.

[15] C. Kaiteris and W. L. Rubin, "Pulse Trains with Low Residue Ambiguity Surfaces That Minimize Overlapping Target Echo Suppression in Limiting Receivers," Proc. IEEE **54**, 438–439 (1966).

[16] J. B. Resnick, "High Resolution Waveforms Suitable for a Multiple Target Environment," M.Sc. Thesis, Massachusetts Institute of Technology, June 1962.

[17] R. H. Barker, "Group Sychronization of Binary Digital Systems," in *Communication Theory* (W. Jackson, Ed.), Academic Press, New York, 1953.

[18] R. Turyn, "On Barker Codes of Even Length," Proc. IRE **51**, 1256 (1963).

[19] E. N. Fowle, "The Design of Radar Signals," Mitre Corp. Report SR-98, November 1, 1963, Bedford, Mass.

[20] S. W. Golomb, "Sequence with Randomness Properties," Glenn L. Martin Co., Internal Report, Baltimore, June 1955.

[21] D. A. Huffman, "The Synthesis of Linear Sequential Coding Networks," in *Information Theory* (C. Cherry, Ed.), Academic Press, New York, 1956.

[22] N. Zierler, "Several Binary-Sequence Generators," Technical Report No. 95, Massachusetts Institute of Technology, Lincoln Laboratory, September 1955.

[23] W. W. Peterson, *Error Correcting Codes*, Massachusetts Institute of Technology Press, Cambridge, Mass., 1961.

[24] B. Elspas, "The Theory of Autonomous Linear Sequential Networks," IRE Trans. **CT-6**, 45–60 (March 1959).

[25] M. P. Ristenblatt, "Pseudo-Random Binary Coded Waveforms," Chapter 4 in [9-4].

[26] T. G. Birdsall and M. P. Ristenblatt, "Introduction to Linear Shift-Register Generated Sequences," Cooley Electronics Laboratory, Technical Report No. 90, University of Michigan Research Institute, October 1958.

[27] S. Golomb (Ed.), *Digital Communications*, Prentice-Hall, Englewood Cliffs, N.J., 1964.

[28] S. E. Craig, W. Fishbein, and O. E. Rittenbach, "Continuous-Wave Radar with High Range Resolution and Unambiguous Velocity Determination," IRE Trans. PGMIL 153–161 (April 1962).

[29] W. Fishbein and O. E. Rittenbach, "Correlation Radar Using Pseudo-Random Modulation," 1961 IRE Int. Conv. Rec. Pt. 5, pp. 259–277.

[30] R. S. Berkowitz, *Modern Radar: Analysis, Evaluation and System Design*, Wiley, New York, 1965.

[31] D. Huffman, "The Generation of Impulse-Equivalent Pulse Trains," IRE Trans. Information Theory **IT-8**, S10–S16 (Sept. 1962).

[32] S. W. Golomb and R. A. Scholtz, "Generalized Barker Sequences," IEEE Trans. Information Theory **IT-11**, 533–537 (1965).

[33] R. C. Heimiller, "Phase Shift Codes with Good Periodic Correlation Properties," IRE Trans. **IT-7**, 254–257 (1961).

[34] R. L. Frank, "Polyphase Codes with Good Nonperiodic Correlation Properties, IEEE Trans. **IT-9**, 43–45 (1963).

[35] T. Sakamoto, Y. Taki, H. Miyakawa, H. Kobayashi, and T. Kanda, "Coded Pulse Radar System," J. Faculty Eng. Univ. Tokyo **27**, 119–181 (1964).

[36] H. Urkowitz, C. A. Hauer, and J. F. Koval, "Generalized Resolution in Radar Systems, Proc. IRE **50**, No. 10, 2093–2105 (1962).

[37] C. A. Stutt, "A Note on Invariant Relations for Ambiguity and Distance Functions," IRE Trans. **IT-5**, 164–167 (Dec. 1959).

[38] W. L. Root, Paper presented at IDA Summer Study, 1963.

[39] C. W. Helstron, *Statistical Theory of Signal Detection*, Pergamon Press, New York, 1960.

[40] F. B. Reis, "A Linear Transformation of the Ambiguity Function Plane," IRE Trans. Information Theory **IT-8**, 59 (1962).

[41] C. H. Wilcox, "A Mathematical Analysis of the Waveform Design Problem," General Electric Co., Schenectady, N.Y., Report No. R57EMH54, October 1957.

[42] C. H. Wilcox, "The Synthesis Problem for Radar Ambiguity Functions," Mathematics Research Center, University of Wisconsin, MRC Technical Summary Report No. 157, April 1960.

[43] C. A. Stutt, "The Application of Time/Frequency Correlation Functions to the Continuous Waveform Encoding of Message Symbols," WESCON, Sect. 9-1, 1961.

[44] C. A. Stutt, "Some Results on Real Part/Imaginary Part and Magnitude/Phase Relations in Ambiguity Functions," IEEE Trans. Information Theory **IT-10**, No. 4, 321–327 (Oct. 1964).

[45] E. A. Guillemin, *Mathematics of Circuit Analysis*, Technology Press, Cambridge, Mass., and Wiley, New York, 1949.

[46] J. Klauder, "The Design of Radar Signals Having Both High Range Resolution and High Velocity Resolution," Bell Syst. Tech. J. **39**, 809–819 (1960).

[47] C. W. Helstrom, "The Resolution of Signals in White Gaussian Noise," Proc. IRE **43**, 1111–1118 (Sept. 1955).

[48] W. L. Root, "Radar Resolution of Closely Spaced Targets," IRE Trans. PGMIL **MIL-6**, No. 2 (April 1962).

[49] B. Elspas, "A Radar System Based on Statistical Estimation and Resolution Considerations," Stanford Electronics Laboratories, Stanford University, Technical Report No. 361-1, August 1, 1955.

[50] J. Allan, M. S. Thesis, Department of Electrical Engineering, Massachusetts Institute of Technology,

[51] P. Swerling, "The Resolvability of Point Sources," Proc. Symp. Decision Theory, Rome Air Development Center, Rome, N.Y., Technical Report No. 60-70A, April 1960.

[52] N. J. Nilsson, "On the Optimum Range Resolution of Radar Signals in Noise," IRE Trans. Information Theory **IT-7**, 245–253 (Oct. 1961).

[53] I. Selin, "Estimation of the Relative Delay of Two Similar Signals of Unknown Phases in White Gaussian Noise," IEEE Trans. Information Theory **IT-10**, No. 3, 189–191 (1964).

[54] E. Brookner, "Optimum Clutter Rejection," IEEE Trans. Information Theory **IT-11**, No. 4, 597–598 (Oct. 1965).

[55] H. Urkowitz, "Filters for the Detection of Small Radar Signals in Noise," J. Appl. Phys. **24**, 1024–1031 (Aug. 1953).

[56] E. L. Key, E. N. Fowle, and R. D. Haggerty, "A Method of Designing Signals of Large Time-Bandwidth Product," 1961 IRE Int. Conv. Rec. Pt. 4, pp. 146–154.

[57] D. A. George, "Matched Filters for Interfering Signals," IEEE Trans. Information Theory **IT-11**, No. 1 (Jan. 1965).

[58] F. C. Schweppe and D. L. Gray, "Radar Signal Design Subject to Simultaneous Peak and Average Power Constraints," IEEE Trans. Information Theory **IT-12**, No. 1, 13–26 (Jan. 1966).

[59] M. G. Lichtenstein and T. Y. Young, "The Resolution of Closely Spaced Signals," IEEE Trans. Information Theory **IT-14**, No. 2, 288–293 (March 1968).

[60] P. M. Woodward, *Probability and Information Theory, with Application to Radar*, Pergamon Press, New York, 1953.

[61] R. W. Lucky, "Techniques for Adaptive Equalization of Digital Communication Systems," Bell Syst. Tech. J. 255–286 (Feb. 1966).

[62] M. J. DiToro, "A New Method of High-Speed Adaptive Serial Communication through Any Time-Variable and Dispersive Transmission Medium," First IEEE Ann. Commun. Conv., Boulder, Colo., Conv. Rec., p. 763.

[63] M R. Aaron and D. W. Tufts, "Intersymbol Interference and Error Probability," IEEE Trans. **IT-12**, No. 1 (Jan. 1966).

[64] I. Gerst and J. Diamond, "The Elimination of Intersymbol Interference by Input Signal Shaping," Proc. IRE **49**, 1195–1203 (1961).

[65] P. A. Bello, "Joint Estimation of Delay, Doppler, and Doppler Rate," IRE Trans. Information Theory **IT-6**, No. 3, 330–341 (June 1960).

[66] E. J. Kelly, "The Radar Measurement of Range, Velocity, and Acceleration," IRE Trans. Mil. Elec. **MIL-5**, 51–57 (April 1961).

[67] F. C. Schweppe, "Radar Frequency Modulations for Accelerating Targets under a Bandwidth Constraint," IEEE Trans. Mil. Elec. **MIL-9**, 25–32 (Jan. 1965).

[68] R. deBuda, "An Extension of Green's Condition to Cross-Ambiguity Functions," IEEE Trans. Information Theory **IT-13**, No. 1, 75–82 (Jan. 1967).

[69] E. J. Kelly and R. P. Wishner, "Matched-Filter Theory for High-Velocity Targets," IEEE Trans. Mil. Elec. **MIL-9**, 56–69 (Jan. 1965).

[70] R. L. Gassner and G. R. Cooper, "Note on a Generalized Ambiguity Function," IEEE Trans. Information Theory **IT-13**, 126 (Jan. 1967).

[71] D. A. Swick, "Wideband Ambiguity Function of Pseudo-Random Sequences: An Open Problem," IEEE Trans. Information Theory **IT-14**, 602–603 (1968).

[72] J. M. Speiser, "Wide-Band Ambiguity Functions," IEEE Trans. Information Theory **IT-13**, 122–123 (Jan. 1967).

[73] R. J. Purdy and G. R. Cooper, "A Note on the Volume of Generalized Ambiguity Functions," IEEE Trans. Information Theory **IT-14**, No. 1, 153–154 (Jan. 1968).

[74] E. L. Titlebaum, "A Generalization of a Two-Dimensional Fourier Transform Property for Ambiguity Functions," IEEE Trans. Information Theory **IT-12**, No. 1, 80–81 (Jan. 1966).

[75] C. W. Helstrom, "An Expansion of a Signal in Gaussian Elementary Signals," IEEE Trans. Information Theory **IT-12**, No. 1, 81–82 (Jan. 1966).

[76] R. Manasse, "Range and Velocity Accuracy from Radar Measurements," Massachusetts Institute of Technology, Lincoln Laboratory, Group 312–26, February 1955.

[77] E. J. Kelly, I. S. Reed, and W. L. Root, "The Detection of Radar Echoes in Noise. I and II," J. SIAM **8**, 309–341, 481–507 (1960).

[78] P. Swerling, "Parameter Estimation Accuracy Formulas," IEEE Trans. Infor. Thy., **IT-10,** No. 1, 302–313 (Oct. 1964).

[79] R. J. McAulay and E. M. Hofstetter, "Barankin Bounds on Parameter Estimation Accuracy Applied to Communications and Radar Problems," Massachusetts Inst. of Tech. Lincoln Laboratory Technical Note 1969-20, March 13, 1969.

[80] R. J. McAulay and L. P. Seidman, "A Useful Form of the Barankin Lower Bound and its Application to PPM Threshold Analysis," IEEE Trans. on Info. Thy., **IT-15,** 273–279 (March 1969).

[81] A. B. Baggeroer, "The Barankin Bound on the Estimation of Parameters Imbedded in the Covariance of a Gaussian Process," Proc. M. J. Kelly Conf. on Comm., Univ. of Missouri at Rolla, Oct. 6–8, 1970.

[82] M. Zakai and J. Ziv, "On the Threshold Effect in Radar Range Estimation," IEEE Trans. on Info. Thy., **IT-15,** 167–170 (Jan. 1969).

[83] J. Ziv and M. Zakai, "Some Lower Bounds on Signal Parameter Estimation," IEEE Trans. on Info. Thy., **IT-15,** 386–392 (May 1969).